Study of sorption properties of Eu on MX-80 bentonite under highly saline, reducing conditions, and under saline, reducing conditions

SORPTION STUDY OF SORPTION PROPERTIES OF Eu (III)

ON MX-80 BENTONITE

UNDER HIGHLY SALINE, REDUCING CONDITIONS, AND SALINE,

REDUCING CONDITIONS

By JIECI YANG, B.Eng.

A THESIS

SUBMITTED TO THE DEPARTMENT OF ENGINEERING PHYSICS

AND THE SCHOOL OF GRADUATE STUDIES

OF MCMASTER UNIVERSITY

IN PARTIAL FULFILMENT OF THE REQUIREMENTS

FOR THE DEGREE OF

MASTER OF APPLIED SCIENCE

Master of Applied Science (2021) McMaster University

(Engineering Physics) Hamilton, Ontario, Canada

TITLE:	Study of sorption properties of Eu on MX-80 under highly saline, reducing conditions, and saline, reducing conditions
AUTHOR:	Jieci Yang B.Eng. (Engineering Physics) McMaster University, Hamilton, Canada
SUPERVISOR:	Dr. Shinya Nagasaki
NUMBER OF PAGES:	x, 58

Abstract

Pu (III) is one of the key elements in the safety assessments of Canadian deep geological repository program (DGR). Sorption is a potential mechanism for retarding radionuclide transport from a DGR to the environment. In the current scenario, Pu (III) is considered to be a dominant radioactive element in the deep geological groundwater. Eu, considered to be a chemical analogue of Pu (III), its sorption behavior is now the target of our research.

This thesis investigates the sorption properties of Eu on MX-80 under saline reducing conditions, and highly saline reducing conditions. The thermodynamic sorption modelling of Eu is also need to be applied. A surface sorption model is also developed by applying computer program for Eu (III) on MX-80 to investigate the sorption mechanisms of Eu (III) sorption.

Acknowledgements

I would like to thank my supervisor, Dr. Shinya Nagasaki, and our collaborating researchers from the JAEA, 1, 2, and 3, for all of their help and guidance throughout my time at McMaster and the JAEA. I would also like to thank my colleagues, Josh Racette and Andrew Walker, for all of their helpful discussions and assistance with completing experiments. Finally, I would also like to thank my friends and family, and all other colleagues, for their continued support throughout my research and the writing of this thesis.

I would also like to thank Tammy Yang and Monique Hobbs from the NWMO for reviewing conference papers, as well as this thesis, and providing useful comments.

This research was funded by the Nuclear Waste Management Organization.

Abbreviations

APM	Adoptive Phased management
CPS	counts per second value
DGR	Deep geological repository
DI	Deionized water
GRG	Geoscientific Review Group
HCB	Highly compacted bentonite
ICP-MS	Inductively coupled plasma mass spectroscopy
JAEA	Japan Atomic Energy Agency
NWMO	Nuclear Waste Management Organization
PHREEQC	PH REdox EQuilibrium in C
SCM	The Surface Complexation model
SIT	Specific-ion Interaction Theory
TDB	Thermodynamic Database
TRLFS	Time- resolved Laser-induced Fluorescence spectroscopy
XAFS	X-ray absorption fine structure
XANES	X-ray absorption spectroscopy
2SPNE SC/CE	2 site protolysis non electrostatic surface complexation and cation exchange

Nomenclature

$\mathbf{a_{ion}}$	the activity of the free concentration of the selected ion
$\mathbf{a_j}$	the activity of the free concentration of the selected j ion
$\mathbf{C_{eq}}$	Equilibrium concentration of an ion in solution
$\mathbf{C_i}$	Initial concentration of an ion in solution
I	Ionic strength
L	volume of liquid
$\mathbf{m_N}$	Concentration of the Nth species of ion
$\mathbf{m_{ion}}$	Actual concentration of the selected ion
$\mathbf{m_j}$	the molality of species j
$\boldsymbol{\gamma_{ion}}$	Free Ion Activity Coefficient
$\boldsymbol{\gamma j}$	Free activity Coefficient of the selected j ion
S	Mass of solid
z_N	Charge of the Nth ion.
z_i	Charge of the selected i ion.
ϵ_{jk}	the interaction coefficient between species j and k

Contents

List of Table

List of Figure

1. Introduction

1.1. Background

The Adaptive Phased Management Geoscientific Review Group (APM-GRG; abbreviated to GRG) was established by NWMO in 2012. It aims to provide independent review comments and advice on the preliminary geoscientific assessments being conducted as part of NWMO's evaluations to identify a suitable deep geological repository (DGR) site for Canada's used nuclear fuel in an informed and willing host community (Alexander, 2020).

Until December 2020, the DGR site selection is processing well. Shown in Figure 1, currently there are 2 communities remain in the site selection list, Ignace and South Bruce (Alexander, 2020). For DGR, they have different underground environment: Ignace on crystalline rock and South Bruce on sedimentary rock. And, there are many aspects to consider when deciding the final location.

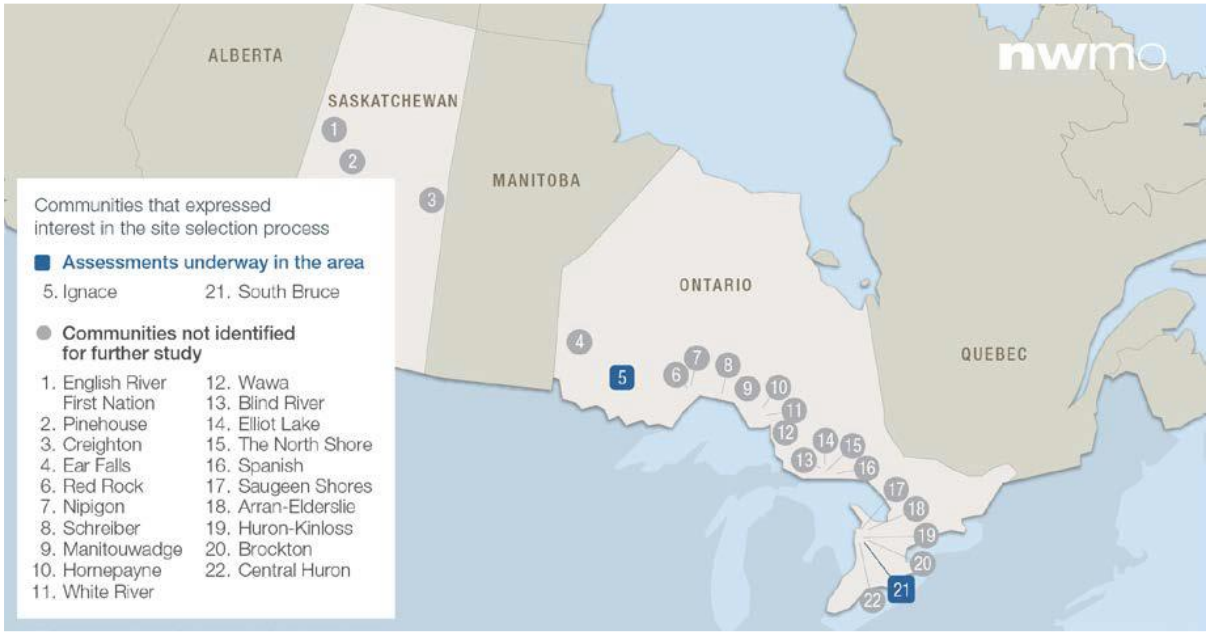

Figure 1: DGR site selection process (Alexander, 2020)

An overview of DGR is shown in figure 2. As what it shows, DGR have a multiple-barrier system which is designed to safely storage the used nuclear fuel over the long term. The facilities on the surface will repackaged the used nuclear fuel into containers, encased in buffer box and transferred to underground placement which is approximately 500 meters. The buffer box will be arranged in the horizontal placement rooms, and backfilled the bentonite solid. (Wayne Robbins, 2020). So, the bentonite solid is one of the main concern in this research.

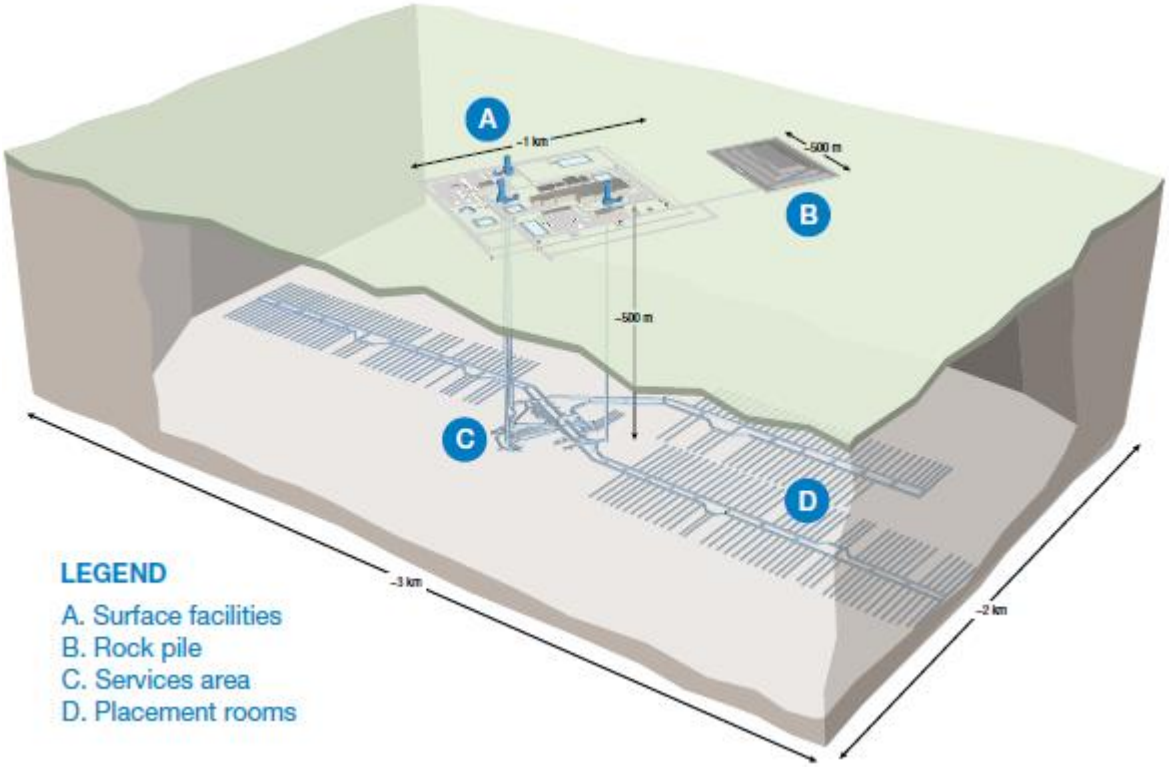

Figure 2: Overview of DGR (Wayne Robbins, 2020)

Figure 3 explains the multiple-barrier system with more detail. As what it shows, the first barrier is the fuel pellet, which is ceramic made by baked uranium dioxide powder. The second barrier is the Zircaloy fuel bundle, The third barrier is a copper-coated steel container, which have enough strength, heat resistance and corrosion resistance to keep the used fuel long enough until its radioactivity decreases to safety levels. The fourth barrier is a highly

compacted bentonite (HCB) clay buffer box, and the fifth barrier is the rock structure nearby (Wayne Robbins, 2020). The multiple-barrier system will protect the DGR from natural events, underground water affects and human activity. The fifth barrier is related with the underground environment in each plan location.

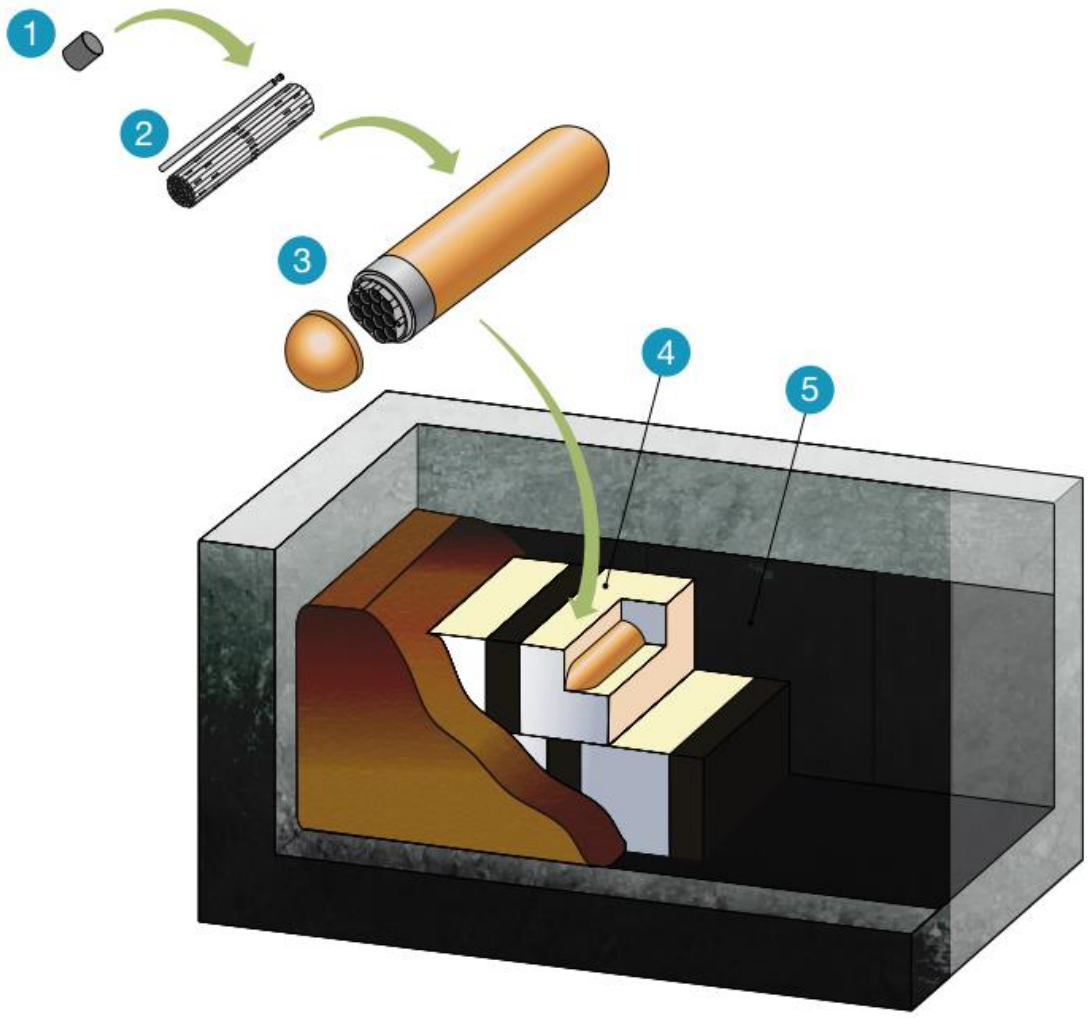

Figure 3: Multiple-barrier system (Wayne Robbins, 2020)

The fourth barrier is related with the topic of this research. As the fourth barrier, the HCB has widely range of use. Its swelling characteristics blocked the migration of radionuclide and provide support for the whole frame. Its low permeability inhibits the porewater flow and its sorption properties inhibit the possible radionuclide movement during

the possible leakage. The bentonite also helps to transfer the heat produced by the storage used fuel bundle (J. Chen, 2020). The MX-80 bentonite, as one of the HCB, will be used in DGR project, and its potential mechanism for retarding Eu transport is studied.

Figure 4: Shaped HCB block

Figure 5: Shaped HCB block with container.

Plutonium, due to its radiotoxicity and long half life, becomes an important element that need to be considered in the deep geological repository project. In radioactive fuel storage research, Pu-239, Pu-240 and Pu-242 are important isotopes. Pu is existed as the states of Pu (III), Pu (IV), Pu (V) and Pu (VI). Among those states, Pu(V) and Pu (VI) are the main existence under oxidizing conditions, and Pu (III) and PU(IV) are the main existence under reducing conditions, which is deeply relevant with the deep geological repository project. For plutonium, on the one hand, is not easy to directly to obtain and used in the experiment. On the other hand, plutonium has special properties to allows the researchers to

contact the researches without use it directly in the experiment. By checking the electron configuration of the elements, which is shown in figure 6: Pu [Rn]$5f^6 7s^2$, Am [Rn]$5f^7 7s^2$, Cm [Rn]$5f^7 6d^7 s^2$, and Eu [Xe]$5f^6 7s^2$, proves the similarity between Pu (III), Am (III), Cm (III) and Eu (III), which lots of evidence has show that 5f and 6d orbitals being involved in covalent bonding to a degree that is similar to that of d-orbitals in transition metal complexes. (M. J. Polinski 2014). The research of H. Rameback (1994) shows the Pu (III), Am (III), Cm (III) and Eu (III) has similar mobility behavior from the nuclear fuel (UO_2) to the compacted bentonite. The research of B. Grambow (2006) proves the Pu (III), AM (III), Cm (III) and Eu (III) have similar pH dependence for the sorption behavior onto MX-80 bentonite, and demonstrated the similarity of sorption behavior of Pu (III), Am (III), Cm (III) and Eu (III) on MX-80 in underground condition. The research of M. Marques Fernandes (2016) measures the sorption isotherm of Eu (III) and Am (III), proves the contribution of the surface species on the strong site and the weak site on the surface sorption of Eu (III) and Am (III) on montmorillonite, and proved that in lower concentration of Eu (III) and Am (III), the strong site surface sorption becomes the majority sorption reaction. Those researches have proved the Am (III), Cm (III) and Eu (III) has the similar sorption behavior, and can be considered to be chemical analogue of Pu (III).

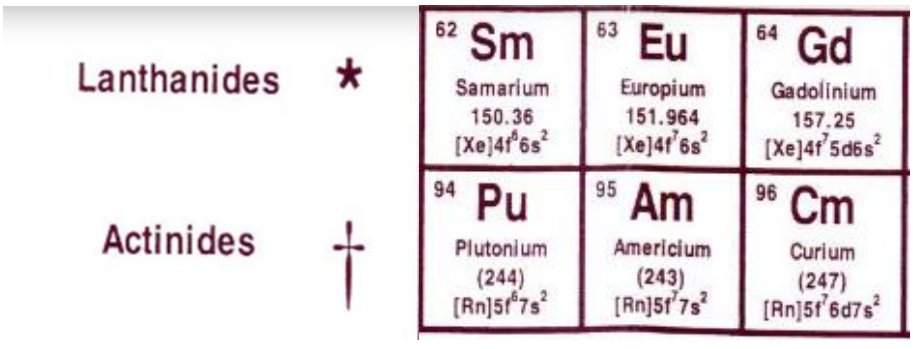

Figure 6: A part of period table of elements

In the current scenario, Eu (III), considered to be a chemical analogue of Pu (III), is the main element that used in this experiment. The only state of element Eu has is the Eu

(III), and that will make it easier to research the sorption behavior of Pu (III) by research the Eu (III) sorption behavior. Also, compare with Pu, Eu is much easy to obtain and use in the laboratory, making the Eu a more realistic choice. In this research, the target is to study the sorption of Eu on MX-80 bentonite under underground environment, which is highly saline, reducing conditions.

A sorption model is also created to simulate the sorption behavior of Eu (III) on MX-80 bentonite in highly saline, reducing conditions. The computer program PHREEQC is used to develop the sorption model, with the reference from Japan Atomic Energy Agency (JAEA) Thermodynamic Database (TDB) and many other researches. The sorption model has ability to describe the sorption behavior of Eu in different soil/underground water flow ratio, pH, ionic strength, the sodium/calcium ion ratio and other conditions on various of solids. And, the parameters of four kinds reference of groundwater (SR-270-PW, CR- 10, CR-10NF and CR- 0) and solutions that uses in the experiment (Na-Ca-Cl and Ca-Na-Cl solutions) have been determined and input into the model.

1.2 Literature review

1.2.1 Review of Available Sorption Data

The use of available sorption data is mainly focusing on the solubility, sorption kinetics, sorption of pH and ionic strength dependence of Eu (III), Am (III) and Cm (III) onto various kind of bentonite.

Zhijun Guo (2009) researches Eu (III) adsorption/ desorption, and Tao Yu (2012, 2019) researches Eu (III) and Am (III) on Na-bentonite. Parveen K. Verma (2019) researches Eu (III) sorption on FEBEX bentonite, Kutch bentonite and Khakassia bentonite. B. Grambow (2005) researches Eu (III) sorption on Ca-montmorillonite in 0.066M Ca (SO3)2 solution, Am on Na montmorillonite and Cm on MX-80 bentonite. A. Bauer (2004)

researches Eu (III) sorption onto smectite. Lu Songshen (2011) and Zhao Sun et al (2019) discover the long-term sorption performance of Eu (III) on Gaomiaozi bentonite, and Pengyuan Gao discover the dependence of Am (III) sorption behavior by the effect of pH and the initial Am (III) and on Gaomiaozi bentonite. Parveen (2019) researches the Eu (III) sorption onto Kutch bentonite, FEBEX bentonite and Khakassia bentonite. E. Tertre. (June 2006), Yukio Tachi (2014), Madhuri A. Patel (2017) researches Eu sorption onto montmorillonite. In Eric's (2002) research, it discovered the sorption of Cm (III) with pH dependence on bentonite (used in DGR), and uses spectroscopic measurements to determine the difference of surface complex production by sorption of Cm (III) on bentonite, Al_2O_3 and SiO_2. One thing that worth to mention is, the influence of microorganisms on migration and sorption process of Cm (III) and Eu (III) on DGR sorption materials has some results achieved, in the research of Miguel A. Ruiz-Fresneda (2020) it shows the Cm (III) and Eu (III) sorption on bentonite (used in DGR) in underground reducing conditions, and detect the production species by XRFS and TRLFS. H, moll's research also studies the D. äspöensis with Cm (III), and detect the production species by TRLFS.

The research about MX-80 bentonite gets more concerned, especially the research data about Eu (III) sorption onto MX-80, the result can be more reliable to compare with the experiment and modelling result. C. Hurel & N. Marmier (2010) researches Eu (III) with high concentration (10^{-5} mol/L) sorption on MX-80 bentonite. Xiangxue Wang (2015) researches Eu (III) sorption on MX-80 bentonite in low ionic strength (0.001 ~ 0,1M) solution. G.D. Shao researches Eu (III) high concentration ($2*10^{-5}$ mol/L) sorption on MX-bentonite in low ionic strength (0.01M $NaClO_4$). Yong He (2020) researches the effect of contact time range 0 – 100min, pH range 4.5 – 7 and temperature range 298 – 318 k, on Eu (III) sorption onto MX-80 bentonite. Yukio Tachi (2014), C. Hurel (2010) and B. Grambow (2006) researched the ionic exchange of Eu (III) on MX-80 bentonite. However, none of the research involves

the Eu (III) low concentration sorption on MX-80 under highly saline, reducing conditions.

1.2.2 TRLFS and XAFS reference data

The Time- resolved Laser-induced Fluorescence spectroscopy (TRLFS) is widely used in probing the strength, composition, and symmetry of the first coordination shell of multiple actinides and lanthanides. The measurement can be proceeded in solution of aqueous complexes, which is very useful for this experiment, and the detection limit for detection concentration, for Cm (III) has determined to be lower than 10^{-9} M. The TRLFS is not been used to detect Eu (III) in this experiment, but the related data can be referenced from other researches, and be used in the discussion section. Also, X-rays absorption fine structure (XAFS) spectra are also used to determine the Eu (III) surface complex species. By analyzing the XAFS, information can be acquired on the local structure and on the unoccupied local electronic states.

Xiangxue Wang (2015)'s TRLFS research has shown in the figure below. It shows the Eu (III) in aqueous bentonite suspension in 0.1M $NaClO_4$ at various pH, which is close to the experiment that proceed in this research. From the ratio of emission intensities of $^5D_0$ ->$^7F_1$/$^5D_0$ ->$^7F_2$ table, with the increase of pH, the intensity ratio decreases, and it means more surface complexation reaction is processing, since the intensity ratio linked to the number of hydration water molecules. The time dependence of fluorescence emission decay figure shows the increase of lifetime of Eu (III) with the increase of pH, and according to Xiangxue Wang and other researcher's calculations, since the lifetime of Eu (III) increases from 105±10 μs at pH 2.7 – 2.05 to (120±10) and (240±10) μs at pH >7, the increases of lifetime is causes by hydration water, and the number of molecule in the first coordination sphere decreases from 9 for the free Eu^{3+} ion at low pH to 4±1 at high pH, meaning the outer sphere complexation is replaced by inner sphere complexation, in higher pH conditions. This

TRLFS result shows with the increases of pH, the sorption of Eu (III) onto bentonite increases, with the increases of the inner-sphere complexation.

Table 1: The spectroscopy characteristics, from Xiangxue Wang (2015).

pH	2.67	3.99	5.03	5.80	6.50	7.15	10.11
$^7F_1/^7F_2$	2.03	1,87	1.24	0.92	0.90	0.88	0.78
τ (μs)	105	105	105	105+240	105+240	120+240	120+240

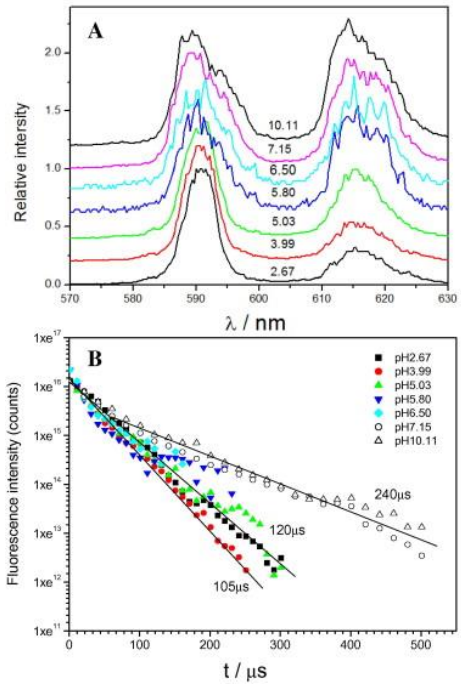

Figure 7: TRLFS result from Xiangxue Wang (2015). for Eu (III) in aqueous bentonite suspensions, the Fluorescence emission spectra and the time dependence of fluorescence emission decay.

A Bauer (2005)'s TRLFS research has also shown in the figure below. It shows the fluorescence emission lifetime of Eu (III) with and without smectite. The similar result as Xiangxue Wang's research is get: inner-sphere complexation is formed when pH rises.

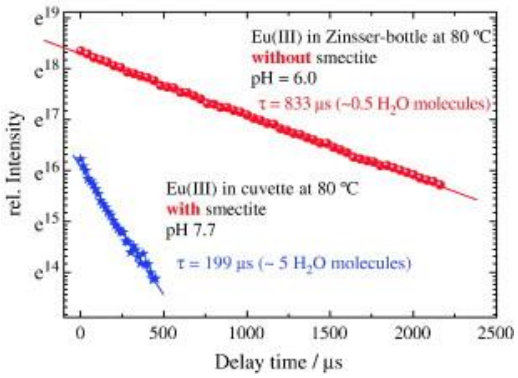

Figure 8: TRLFS results from A Bauer (2005)'s research. The fluorescence emission lifetime of Eu (III) with and without smectite

Parkeen. Kumar. Verma (2016)'s TRLSF research has shown below. It gives a reference of how Eu (III) sorption onto kaolinite, which is a solid that similar with MX-80 bentonite.

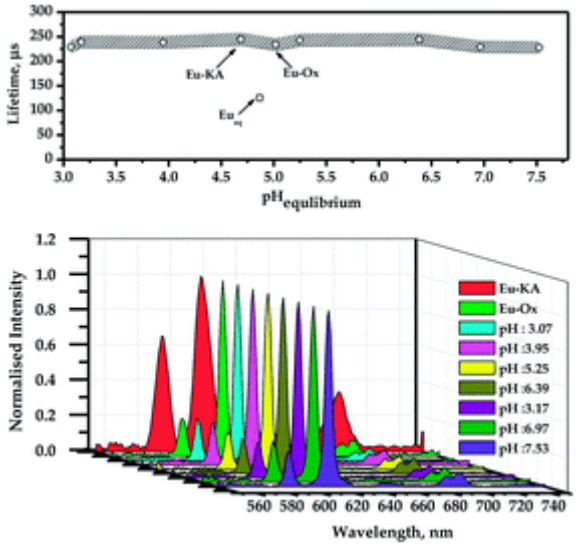

Figure 9: Lifetime and luminescence spectra from Parkeen, Kumar. Verma (2016)'s research, of Eu (III) (concentration 10-4M) sorption onto kaolinite

G. D. Sheng (2009)'s research applied XAFS spectra, and the related research result shows below. The first figure shows the X-ray absorption spectroscopy (XANES) of the Eu-bentonite has shown in low pH environment, the main species of Eu (III) in Eu-bentonite

solution is Eu^{3+}, rather than Eu_2O_3, since the curve of pH =3.41, 2.48 and 1.54 are fits with Eu^{3+}(aq), but have differ position of both peaks of Eu_2O_3. The second figure shows the first-shell fit of the XAFS sorption samples, and further proved in the low pH environment, the Eu^{3+} is the main species of Eu (III) in the solution.

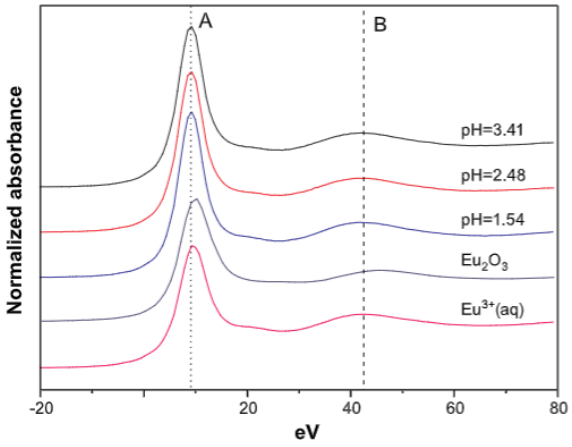

Figure 10: XANES of Eu-bentonite samples, from G. D. Sheng (2009), with Eu (III) concentration 4.72e-3mol, I= 0.01M $NaClO_4$

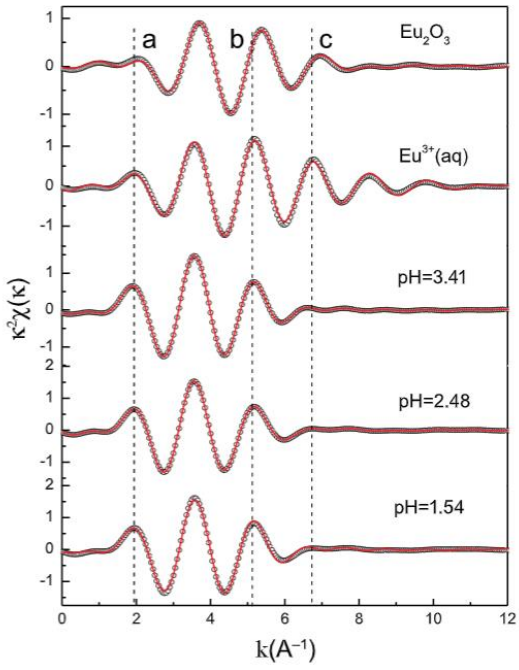

Figure 11: The first-shell fit of the XAFS sorption samples, from G. D. Sheng (2009)'s research

Another research from Jun Hu (2010) also applied XAFS spectra, and shows the similar result as G. D. Sheng already proved: in low pH condition (with HA, in this experiment), the Eu^{3+} are the main species of Eu (III), rather than Eu (OH)3 or Eu_2O_3. There is no related XAFS research found about Eu (III) species in high pH condition.

1.3 Purpose

The purpose of this research is to obtain sorption data for Eu (III) on MX-80 bentonite under Canadian underground sedimentary rock environment. The sorption coefficient for Eu on bentonite in SR-270-PW reference solution will be measured. Also, the sorption dependence on ionic strength and pH will be evaluated, for 0.1, 0.5, 1, 2, 4, 6 M with pH at 3,4,5,6,8,9,10 in Na-Ca-Cl solution, with Na/Ca ratio 2.7. It is required by NWMO, Eu is an important chemical analogue for trivalent actinides, and the related research can help to evaluate the safety assessment for the Canadian DGR.

The sorption modelling of Eu (III) onto bentonite, within SR-270-PW, Na-Ca-Cl and Ca-Na-Cl environments will be established. The sorption model helps to investigate the sorption mechanisms of Eu (III) on various rock. The experimental data will be used to develop the complexation constants for surface complexation reactions. Then, the strong agreement between the model and experiment result demonstrates that the sorption model describes the main sorption activity in the experiments.

2. Theory

2.1 Sorption Mechanisms

Sorption is the adhesion of chemicals to solid surfaces, which occurs in many natural or engineered systems. Sorption is a broad encompassing, and during the sorption process of Eu (III) it can occurred either physically or chemically, or another way of saying, non-specifical or specifical sorption.

2.1.1 non-specifical sorption

The non-specifical sorption is result from non-specific Van der Waal's forces. Vander Wall's force is relatively weak and that makes sorption very easy to reverse, which make it also named physical adsorption. There is a electrical double layer model to explain that, which is described in figure 6.

In the first model of double layer theory, which is the Helmholtz model, it describes a flat capacitor, which is the surface of the mineral, and it could acquire the charge from either permanent structure charge imbalance or potential-determining reactions (in this research it will be vary with pH, and become negative above a certain pH). The negatively charged surface electrostatic pulls cations and maintain balances. Two layers are formed during this process. The inner layer, also called Helmholtz layer, is consists of a surface monolayer which the total number of adsorbed ions is decided by size and surface area. The diffusion area is another concept that describes in Gouy-Chapman model. In the diffuse layers, the absorbed ions are able to move freely as in the free solution. Combine Helmholtz model and Gouy-Chapman model it gets the stern model, which has both the inner layer and the diffuse layers.

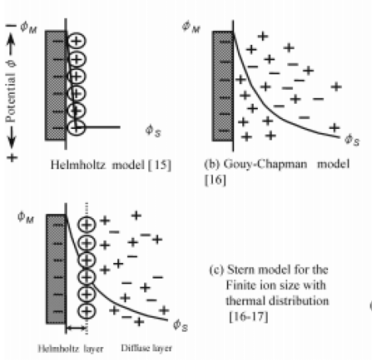

Figure 12: 3 Models of the electrical double-layer at a positively charged surface: (a) the Helmholtz model; (b) the Gouy–Chapman model; and (c) the Stern modelarged surface (Endo.2001)

Non-specific coulombic sorption is reversible with rapid sorption and desorption kinetics. So, it is not considered in this research about DGR that has a very large time span.

2.1.2. Specifical sorption

The specifical sorption is based on the chemical bond between adsorptive and adsorbent species. The chemical bond, explained by quantum theory, is the share or transferred of electrons among two or more nucleus, and build a new equilibrium state. Thus, the specifical sorption is relatively strong, hard to reverse and is highly selective between certain adsorptive and absorbent species. The most common concept to explain specifical sorption is the surface complexation model (SCM).

The surface complexation model explains the metal coordination with surface oxygens atoms, and associate with the surface as an inner or outer sphere complex. As shown in the figure 7, three different complex are coordinated: mononuclear monodentate inner-sphere complex, mononuclear bidentate inner-sphere complex and outer-sphere complex. When forming an inner sphere complex, according to the figure, when forming an inner sphere complex, there is a direct bond between the surface and the adsorbed species; however, in forming an outer sphere complex, it retains its shell of co-ordinated water molecules, and makes it further from the surface nuclear, and causes a weaker sorption

(Payne, 2013). The surface sorption site is to describe the total sorption capacity of the select surface minerals. The sorption sites are usually classified into two kinds: “strong” sites and “weak” sites. “Strong” sites have low capacity but high sorption affinity, and dominate the uptake of adsorbate at low concentration. The inner-sphere complex is more related with “strong” sites since they have relatively strong bonds. “weak” sites have much larger capacity but much lower affinity. The outer-sphere complex is more related with “weak” sites since they have relatively week bonds. For different minerals, the number of surface sites differs significantly, depending on their surface properties.

The strong site sorption has very strong stability, and is importance in the study of absorption of nuclear elements.

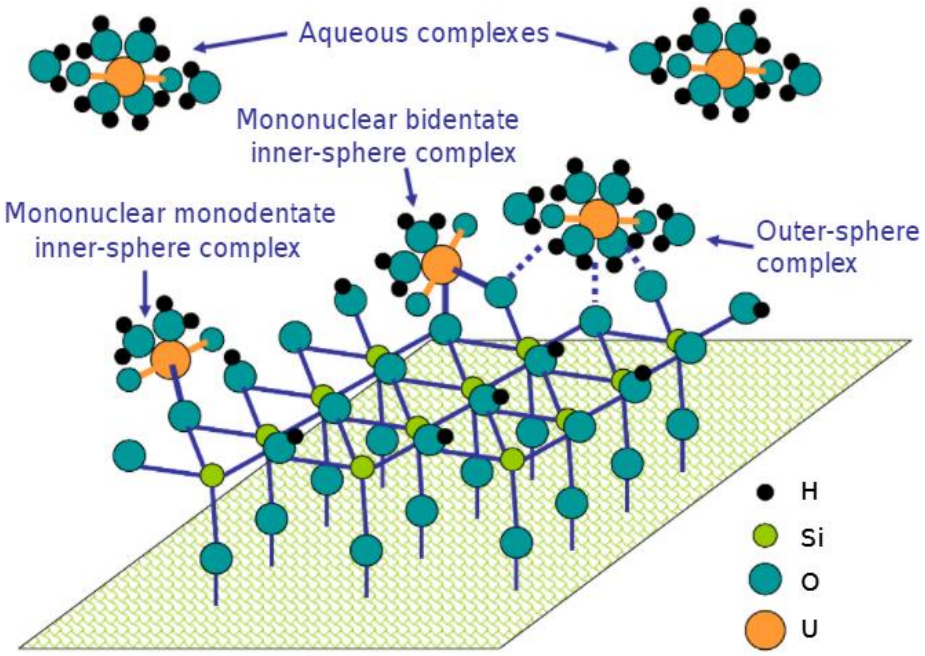

Figure 13: The inner sphere and outer sphere complexes of U(VI) sorption onto a silica surface (Payne, 2013)

There are various surface complex formation equilibria that need to be considered.

According to Aquatic Chemistry: Chemical Equilibria and Rates in Natural Water, set “a” surface hydroxyl group as S-OH, the fictitious metal as Me^{+z}, and fictitious ligand as L^{-y} (Stumm & Morgan, 1996), the equilibria can be express as:

Acid-Base Equilibria:

$$S - OH + H^+ \rightleftharpoons S - OH_2^+$$

$$S - OH \rightleftharpoons S - O^- + H^+$$

Metal Binding:

$$S - OH + M^{2+} \rightleftharpoons S - OM^{(z-1)+} + H^+$$

$$2S - OH + M^{2+} \rightleftharpoons S - OM^{(z-1)+} + 2H^+$$

$$S - OH + M^{2+} + H_2O \rightleftharpoons S - OMOH^{(z-2)+} + 2H^+$$

Ligand Exchange

$$S - OH + L^- \rightleftharpoons S - L + OH^-$$

$$2S - OH + L^- \rightleftharpoons S_2 - L + 2OH^-$$

Temary Surface Complex Formation

$$S - OH + L^- + M^{2+} \rightleftharpoons S - L - M^{z+} + OH^-$$

$$S - OH + L^- + M^{2+} \rightleftharpoons S - OM - L^{(z-2)+} + H^+$$

2.1.3 Ionic exchange

The ionic exchange is a reversible reaction which ions in the solution surrounding the solid are replaced by ions present on an insoluble solid, and have important effect on sorption of Eu on MX-80 bentonite in low pH environment. The ionic exchange is widely occurring during the experiment, such as the pH value and the ionic concentration contains in the reference solutions (SW-270-PW).

The ionic exchange of MX-80 bentonite between Na and other active ions (Eu^{3+}, H^{+}, Ca^{2+}, K^{+}, Mg^{2+}, Ba^{2+}, Sr^{2+}) are considered in modelling, and the equilibria can be express as:

$$X - Na + H^{+} \rightleftharpoons X - H + Na^{+}$$

$$2X - Na + Ca^{2+} \rightleftharpoons 2X - Ca + 2Na^{+}$$

$$3X - Na + Eu^{3+} \rightleftharpoons 3X - Eu + 3Na^{+}$$

2.1.4 The initial concentration of Eu (III)

The initial concentration of Eu (III) determines the initial concentration of Eu species, and for different species they have different sorption behaviors on selected solid, which will influence the experiment result. Also, the initial concentration is expected to set properly, large enough to support the sorption process, and not too large to cover the concentration change by sorption activities.

The initial concentration has effect on sorption behavior of Eu (III) on MX-80 bentonite, which is mainly by its inner-sphere/out-sphere sorption ratio and amounts. In the research of M. H. Bradury (2005), the isotherms for Eu (III) on Na-SWy -1 smectite and Ca-SWy-1 smectite shows the difference of initial concentration of Eu (III) takes effects on the sorption of Eu (III) on smectite. This behavior can be explained by the theory in chapter 2.1.2: the inner-sphere complex is much stable than out-sphere complex, and becomes the main sorption production when Eu concentration is at the low range (under 1E-6 M, in the M.H. Bradury's research). But when the Eu concentration becomes higher, the outer-sphere complex becomes much easier to form and maintain, and it will increase the sorption behavior of Eu (III) on MX-80, which is not be expected to happen in this experiment.

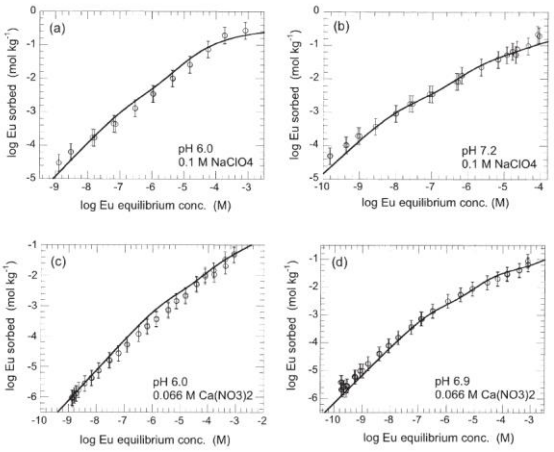

Fig. A8. Sorption isotherms for Eu(III) on Na-SWy-1 (a), (b) and on Ca-SWy-1 (c), (d). The continuous curves are the best fits to the data obtained using the 2SPNE SC/CE model and the non-adjustable parameters given in Table 1, and the fit parameters in Tables 2 to 5.

Figure 14: the isotherms from M. H. Bradury's research, for Eu (III) on Na-SWy-1 and Ca-SWy -1

In another Eu (III) sorption experiment, the isotherm of Eu on MX-80 bentonite shows the Eu (III) sorption status changes with the Eu (III) equilibrium concentration (Bradbury & Baeyens, 2011), which shows the change of equilibrium concentration of Eu (III) only have limited and nonobvious impact on the sorption behaviors of MX-80 bentonite, when the Eu initial concentration is limited in no more than 10E-6 M. And this data will be a very important reference in this experiment.

Time (days)	**S:L ratio** (g L^{-1})	**Equilibrium conc. range** (M)	**pH**
69	1.56	1.6 x 10^{-6} to 3.2 x 10^{-11}	7.4 - 7.6

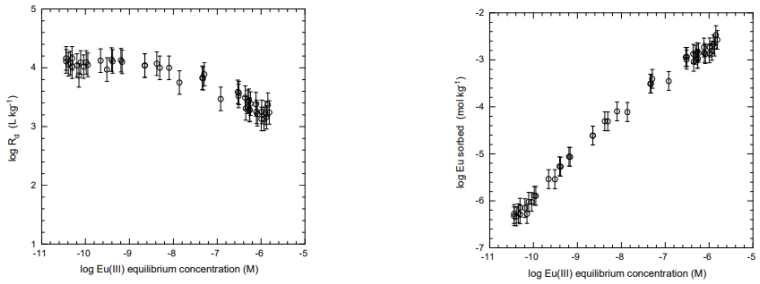

Figure 15: Sorption isotherm of Eu on MX-80 in porewater (Bradbury & Baeyens, 2011)

2.2 Measuring Sorption Experimentally

2.2.1 Sorption experimental method

The currently experimental method is called batch sorption experiment. In Batch experiment, the solid and solution will add into the reaction vessel. As designed, the sorbate in the solution will sorbs into the solid. After it has achieved equilibrium, measure the concentration of sorbate that still remains in the solution, and with this, to determine the sorption capacity of the selected solid

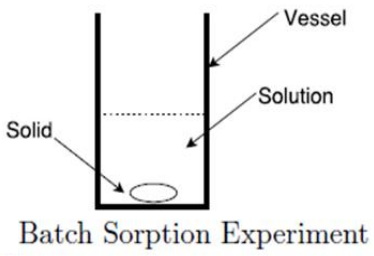

Figure 16: The Batch Experiment (Riddoch, 2016).

2.2.2 Calculation of K_d values

Sorption is usually quantified by sorption distribution coefficients K_d, which is defined as the ratio of sorbate concentration in liquid to the sorbate concentration in solid. Since it is hard to determine the sorbate on solid directly, so distribution coefficient K_d is used by taking the difference between the initial concentration and equilibrium concentration of sorbate in solution. For the K_d calculation, there is also a correction factor to take into account the liquid to solid ratio. K_d is calculated according to equation:

$$K_d = \frac{C_i - C_{eq}}{C_{eq}} \times \frac{L}{S}$$

Where the C_i is the initial concentration of the sorbate in solution, the C_i is the equilibrium concentration of the sorbate in solution, the L is the total volume of liquid, and S is the mass of solid.

2.2.3 Activity corrections

The ions in solution interact to each other, and also interact to water molecules. At low background concentrations, the impact can be ignored; but at higher concentrations ions behave like they are less (or more) than they really are. The activity is quantified by free ion activity coefficient f_i, which takes effect as the follow equation

$$a_{ion} = \gamma_{ion} \times m_{ion}$$

The equation converts the actual concentration of the selected ion (m_{ion}) into the activity of the free concentration of the selected ion (a_{ion}).

The ionic strength (**I**) describes the concentration of the charge in the solution, which is very useful in considering the activity coefficient, and I is calculated by following equation:

$$I = \frac{1}{2}\sum\left(m_N \cdot {Z_N}^2\right)$$

Which m_N represent the concentration of the Nth species of ion, and the Z_N represent the charge of the Nth ion.

After get the ionic strength in the solution, there are several expressions can be used to estimate the activity coefficient for single ion. Each of them can be used in limited range of ionic strength.

For Debye-Huckel (Debye and Huckel, 1923) equations, there is:

$$\log\gamma_j = -A{Z_j}^2 I^{1/2}, \text{for } I < 10^{-2}$$

And the Davies equation (Davies, 1962):

$$\log\gamma_j = -\frac{A{Z_j}^2 I^{1/2}}{1 + a_j \cdot B \cdot I^{1/2}}, \text{for } I < 10^{-1}$$

which A and B have constant value at 25°C: A = 0.51 and B = 0.33×10^{8}. a_j is the ion size parameter. The Z_j represent the charge of the selected ion.

The extended Debye-huckel equation (Truesdell and Jones, 1974) is:

$$\log\gamma_j = -\frac{AZ_j{}^2 I^{1/2}}{1 + Ba_j I^{1/2}}$$

Which a_j is the ion size parameter.

Ion size parameter (cm)	ions
$11\ 10^{-8}$	$Th^{+4}, Zr^{+4}, Ce^{+4}, Sn^{+4}$
$9\ 10^{-8}$	$H^{+}, Al^{+3}, Fe^{+3}, La^{+3}, Ce^{+3}, Cr^{+3}, Sc^{+3}, Y^{+3}, In^{+3}, Pr^{+3}, Nd^{+3}, Sm^{+3}$
$8\ 10^{-8}$	Mg^{+2}, Be^{+2}
$6\ 10^{-8}$	$Ca^{+2}, Zn^{+2}, Cu^{+2}, Sn^{+2}, Mn^{+2}, Fe^{+2}, Ni^{+2}, Co^{+2}, Li^{+}$
$5\ 10^{-8}$	$Ba^{+2}, Sr^{+2}, S^{-2}, Ra^{+2}, Cd^{+2}, Hg^{+2}, S_2O_4^{-2}, WO_4^{-2}$
$4.5\ 10^{-8}$	$Pb^{+2}, CO_3^{-2}, SO_3^{-2}, MoO_4^{-2}$
$4.5\text{-}4\ 10^{-8}$	$Na^{+}, CdCl^{+}, ClO_2^{-}, IO_3^{-}, HCO_3^{-}, HSO_3^{-}, H_2PO_4^{-}, H_2AsO_4^{-}$
$4\ 10^{-8}$	$SO_4^{-2}, HPO_4^{-2}, PO_4^{-3}, Hg_2^{+2}, SeO_4^{-2}, CrO_4^{-2}, S_2O_3^{-2}, S_2O_6^{-2}, S_2O_8^{-2}$
$3.5\ 10^{-8}$	$OH^{-}, F^{-}, NCS^{-}, NCO^{-}, HS^{-}, ClO_2^{-}, ClO_4^{-}, BrO_3^{-}, IO_4^{-}, MnO_4^{-}$
$3\ 10^{-8}$	$K^{+}, Cl^{-}, I^{-}, NO_3^{-}, Br^{-}, CN^{-}, NO_2^{-}$
$2.5\ 10^{-8}$	$Rb^{+}, Cs^{+}, Tl^{+}, Ag^{+}, NH_4^{+}$

Figure 17: The ion size parameter table (Kafumbila, 2020).

The Specific-ion interaction theory (SIT) equation (Grenthe and Plyasunov, 1997). is applied in higher ionic strengths:

$$\log\gamma_j = -\frac{AZ_j{}^2 I^{1/2}}{1 + 1.5 I^{1/2}} + \sum_k \epsilon_{jk}\, m_k$$

Which the ϵ_{jk} is the interaction coefficient between species j and k, and m_k is the molality of species k.

The interaction coefficient between species is get from the SIT theory capable PHREEQC database. The SIT equation is widely applied in this research, since the high

concentration of Na-Ca-Cl and Ca-Na-Cl inhibited the activity of H^+, and impacted the pH value, the activity coefficient of H^+ in high ionic strength solution is need to be figured.

2.3 The PHREEQC Program

PHREEQC version 3 is a computer program written in C and C++ that is designed to perform variety of aqueous geochemical calculations, and has capabilities for speciation and saturation-index calculation, batch-reaction and 1-D transport calculation with reversible and irreversible reaction, specified mole transfers of reactants, kinetically controlled reactions, mixing of solutions, the pressure and temperature changes. The SIT theory is also used in the program.

In PHREEQC, series of database are used with the program: the database derived from PHREEQE (Parkhurst and others, 1980), the database derived from WATEQ4F (Ball and Nordstrom, 1991). The database derived from EQ3/6 and Geochemist's Workbench that uses thermodynamic data compiled by the Lawrence Livermore National Laboratory, the data base derived from the database for the program MINTEQA2 (Allison and others, 1991), the database derived from MINTEQA2 version 4 (U.S. Environmental Protection Agency, 1998), the database for the SIT model of Pitzer (Pitzer, 1973) as implemented in PHRQPITZ (Plummer and others, 1988), the database implementing the SIT by Grenthe and others (Grenthe and others, 1997), and a partial implementation of the individual component by Thorstenson and Parkhurst (Thorstenson and Parkhurst, 2002,2004). During this experiment, for Eu (III) sorption on various of solid, the Eu (III) behavior is not included in the above basement, and the data is quote from other articles.

3. Experimental Methods

3.1 Materials

The MX-80 bentonite sample contains are quartz, feldspar, calcite ($CaCO_3$, (Ca, Fe) CO_3), and pyrite, and was supplied by the American Colloid company, and is ready to be used in the experiment. The MX-80 bentonite is used as a landfill material, and planning to be used in DGR plan, which makes it important in this research. The NaCl, $CaCl_2 \cdot 2H_2O$ solid that is used for adjust the Ionic strength of the solution, The HCl and NaOH solutions that is used to adjust the pH of the solution, were purchased from Fisher Scientifics. The Eu standard solution is obtained from Agilent Technologies in the form of 1000µg/ml Eu in 5% HNO3.

3.2 Preparation of saline solutions

The Na-Ca-Cl saline solutions and Ca-Na-Cl saline solutions are used to build the sedimentary and crystalline underground environment. These solutions are made by NaCl, $CaCl_2 \cdot 2H_2O$, and deionized water. The Na-Ca-Cl saline solutions, which is applying in simulating sedimentary environment, using the Na/Ca ratio of 2.7. The Ca-Na-CL saline solutions, which apply in simulating crystalline environment, using the Na/Ca ratio of 1.35. The different ionic strength of the solution is required, and it determined the mass of each salt used in preparing different solutions, and the related data is listed on the following table:

Table 2: Mass of salt to prepare Na-Ca-Cl and Ca-Na-Cl solutions

Environment	The ionic strength (M)	NaCl (g/L)	CaCl2·2H2O(g/L)
Na-Ca-Cl Solution /Sedimentary environment	0.1	2.768	2.579
	0.5	13.841	12.895
	1	27.682	25.791

	2	55.364	51.582
	4	110.728	103.164
	6	166.092	154.745
Ca-Na-Cl solution /Crystalline environment	0.05	0.9954	1.6155
	0.1	1.9908	3.231
	0.24	4.778	7.7544
	0.5	9.954	16.605
	1	19.908	32.31

Then the Eu standard solution was added into the solution and make the initial concentration of Eu becomes 10^{-6} M and 10^{-7} M. The pH adjustment solution HCl and NaOH was used to adjust pH value.

3.3 Detection limit of Eu by using ICP-MS

The detection limit of Eu describes the lowest concentration that can be measured by ICP-MS, and it is necessary to set the initial concentration of Eu and solid/liquid ratio in the experiment. The calibration of Eu on ICP-MS is using solutions with Eu concentration of 10^{-7}M, 10^{-8}M, 10^{-9}M, 10^{-10}M, 10^{-11}M, 10^{-12}M and 10^{-13}M, and DI water solution. The counts per second (CPS) value of Eu-151 and Eu-153 will be compared with result from DI, and define if that reaches the detection limit.

The calibration experiment of Eu defines the detection limit is below 10^{-13}, since the samples that detected by the ICP-MS in the experiment need to be dilute by DI by the factor of 20, The detection limit of Eu by using ICP-MS can be define as $2*10^{-12}$ or $5*10^{-12}$M.

3.4 The Eu solubility detection

The solubility of Eu determines the highest concentration that is allowed in the experiment. For detecting the solubility of Eu, adding the Eu standard solution into Na-Ca-Cl solutions with ionic strength 0.1M and 6M, and make the solution with Eu concentration of 10^{-4} M, 10^{-6}M, 10^{-7}M and 10^{-8}M. The concentration of Eu remain in solution will be detected

by ICP-MS at day 1, 2, 3, 7,14, 21, and 28 after the solution is manufacture. The result will be collected and used to evaluate the solubility of Eu.

The experiment result shows the stability of concentration of Eu 10^{-6} M, 10^{-7}M and 10^{-8}M during 28 days time period, the solubility of Eu in the experiment condition is higher than 10^{-6}M, and both 10-6M and 10-7M is recommended according to the experiment results, from both solubility experiment and detection limit of Eu in ICP-MS experiment.

3.5 Eu (III) sorption kinetics

To investigate the sorption kinetics of Eu on shale, limestone, bentonite, and illite in brine solutions, under reducing conditions and the sorption kinetics of Eu on granite and bentonite in saline solutions, under reducing conditions are one of the main topics of this research.

The batch sorption experiment is applied. The solid/liquid ratios for all kinetic experiments are 20mg/10mL, the 20mg of shale, limestone, bentonite, illite, and granite is added into the 15mL test tube. Then the following steps is proceeded in the N_2 gas filled glovebox. The pre-equilibration is proceeded, for shale, limestone, bentonite and illite, the Na-Ca-Cl solutions with various ionic strength will be add 10ml into the tube; for granite and bentonite, the Ca-Na-Cl solutions will be added. The suspensions were kept in the N_2 environment for a week for pre-equilibration. Then the liquid is separated by centrifuge (6min at 3000ref) and removed by pipette. Then 10 mL of Na-Ca-Cl or Ca-Na-Cl solutions with Eu concentration of 10^{-6} M is added into the corresponding test tube. In 30 ~ 40 days time period, the upper liquid will be taken 5mL centrifuge (30min at 18000rpm), and take the upper liquid (500μm), dissolve with DI water in 20 times to make the sample for ICP-MS detection.

Since the kinetic behavior is figured, one of the research topics is completed, and it

also provided the necessary data for designing the rest of experiments.

3.6 Ionic strength and pH dependence of Eu (III) sorption

To investigate effects of pH (3-10) and ionic strength (0.1-6M) on the sorption of Eu on shale, limestone, bentonite, illite and granite in brine/saline solutions, under reducing conditions are main topics of this research.

In the experiment, the dependence of pH and ionic strength on bentonite is evaluated in Na-Ca-Cl (Na/Ca ratio is 2.7) solution is investigated by using samples covering pH 3, 4, 5, 6, 8, 9, 10 and ionic strength 0.1M, 0.5M,1M, 2M, 4M and 6M. During the entire experiment the solid/liquid ratio is 10mg/10mL and the initial Eu concentration is 10^{-7} M. The preparation process is similar with Eu sorption kinetics, and after 30 days, take 5mL centrifuge (30min at 18000rpm) and take the upper liquid (500μm), dissolve with DI water in 20 times when ionic strength of the solution is 0.1M and 0.5M, 50 times when ionic strength is 1M, 100 times when 2M, and 200 times when 4M and 6M. This is to avoid the high saline causes crystalline in ICP-MS in appropriate place.

4. Sorption Model

As discussed in 2.3, PHREEQC version 3 is a computer program written in C and C++ that is designed to model the sorption of Eu (III) onto various of rocks in underground environment. In this chapter, it will discuss the detail of the modelling, and explain the essential data.

4.1 Thermodynamic data

The SOLUTION data blocks (appendix B) defined the initial concentration of aqueous master species. In this model there are four different underground solutions: CR-10, CR-10 NF, CR-0 and SR-270-PW. The CR-10, CR-10 NF and CR-0 solution compositions are according to article Sorption Testing for Se, Tc, Np, U and Eu on Crystalline Rocks, and SR-270-PW are according to NWMO report (Peter and Tammy, 2018), and the initial solution concentration that applied in model is shown in Table below:

Table 3:Aqueous species and concentration in the Eu (III) initial solution

	Initial concentration			
Species	CR-10	CR-10NF	CR-0	SR-270-PW
pe/pH	-3.5/7.0	-9.75/8.7	1.53/7	-3.39/6
Na^{+}	0.08265	0.272077	0.00326232	2.179
K^{+}	0.000384	0.002046	0.00007673	0.3197
Ca^{2+}	0.053146	0.021708	0.000998	0.798
Mg^{2+}	0.002469	0.007488	0.000411437	0.3374
$CO3^{2-}$/C (+4)	0.001147	0.000066	0.00377	0.0018028
$SO4^{2-}$/S (+6)	0.01041	0.044908	0.00052	0.00458
Cl^{-}	0.172058	0.1709	0.001128254	4.753

Sr^{-}	0.000285	0.000285	0.000011412	0.0137
F^{-}	0.000105	0.0001	0.0001	0.000105
Eu^{+3}	1E-6/1E-7	1E-6/1E-7	1E-6/1E-7	1E-6/1E-7

The initial concentration of Na-Ca-Cl and Ca-Na-Cl solutions has simpler form, and the data applied in model is shown in Table below:

Table 4:Aqueous species and concentration of experiment solution Ca-Na-Cl

	Initial concentration of Ca-Na-Cl			
Species	Is = 0.05M	Is = 0.1M	Is = 0.24M	Is = 1M
pe/pH	-3.5/6.0	-3.5/6.0	-3.5/6.0	-3.5/6.0
Ca^{2+}	0.010989	0.0221978	0.052747	0.21978
Na^{+}	0.017033	0.0340659	0.081758	0.340659
Cl^{-}	0.028022	0.0562637	0.134505	0.560439

Table 5:Aqueous species and concentration of experiment solution Na-Ca-Cl

	Initial concentration of Na-Ca-Cl					
Species	Is = 0.1M	Is = 0.5M	Is = 1M	Is = 2M	Is = 2M	Is = 2M
pe/pH	-3.5/6.0	-3.5/6.0	-3.5/6.0	-3.5/6.0	-3.5/6.0	-3.5/6.0
Ca^{2+}	0.01754	0.08772	0.17544	0.35088	0.70176	1.05264
Na^{+}	0.047368	0.23684	0.47368	0.94736	1.89472	2.84208
Cl^{-}	0.064908	0.32456	0.64912	1.29824	2.59648	3.89472

The aqueous species that is likely to form based on the aqueous master species is based on their formation reactions, and are shown in the table below.

Table 6: Formation reactions and formation constants of relevant species in the JAEA TDB (Kitamura et al., 2014). and other articles (Tertre E., Berger G, 2016) (Spahiu, K, and Bruno, J. 2015)

Formation reaction	Log K	Error
$H_2O - H^+ \leftrightarrow OH^-$	-14.001	0.015
$2H_2O + 4H^+ + 4e^- \leftrightarrow O_2$	-86.080	
$Ca^{+2} + H_2O - H^+ \leftrightarrow CaOH^+$	-12.850	0.500
$Mg^{+2} + H_2O - \leftrightarrow MgOH^+$	-11.794	
$Sr^{+2} + H_2O - H^+ \leftrightarrow SrOH^+$	-13.290	
$Cl^- + H_2O - H^+ - 2e^- \leftrightarrow ClO^-$	-57.933	0.170
$Cl^- + 2H_2O - 4H^+ - 4e^- \leftrightarrow ClO_2^-$	-107.874	0.709
$Cl^- + 3H_2O - 6H^+ - 6e^- \leftrightarrow ClO_3^-$	-146.238	0.236
$Cl^- + 4H_2O - 8H^+ - 8e^- \leftrightarrow ClO_4^-$	-187.785	0.108
$Cl^- + H_2O - H^+ - 2e^- \leftrightarrow HClO$	-50.513	0.109
$Cl^- + 2H_2O - 3H^+ - 4e^- \leftrightarrow HClO_2$	-105.913	0.708
$HS^- - H^+ \leftrightarrow S^{-2}$	-19.000	2.000
${SO_4}^{-2} - H_2O + 2H^+ + 2e^- \leftrightarrow {SO_3}^{-2}$	-3.397	0.701
${SO_4}^{-2} - 5H_2O + 10H^+ + 8e^- \leftrightarrow {S_2O_3}^{-2}$	38.013	1.985
${SO_4}^{-2} - 4H_2O + 9H^+ + 8e^- \leftrightarrow HS^-$	33.692	0.378
$HS^- + H^+ \leftrightarrow H^2S$	6.990	0.170
${SO_3}^{-2} + H^+ \leftrightarrow {HSO_3}^-$	7.220	0.080
${S_2O_3}^{-2} + H^+ \leftrightarrow {HS_2O_3}^-$	1.590	0.150
$0.5{S_2O_3}^{-2} + 1.5H_2O - H^+ - 2e^- \leftrightarrow H_2SO_3$	-13.344	0.710
${SO_4}^{-2} + H^+ \leftrightarrow {HSO_4}^-$	1.980	0.050
$Ca^{2+} + {SO_4}^{-2} \leftrightarrow CaSO_4$	2.309	

$Mg^{2+} + SO_4{}^{-2} \leftrightarrow MgSO_4$	2.250	
$Na^{+} + SO_4{}^{-2} \leftrightarrow NaSO_4{}^{-}$	0.700	
$K^{+} + SO_4{}^{-2} \leftrightarrow KSO_4{}^{-}$	0.850	
$CO_3{}^{2-} + H^{+} \leftrightarrow HCO_3{}^{-}$	10.329	0.020
$CO_3{}^{2-} + H_2O + 2H^{+} \leftrightarrow CO_2$	16.683	0.028
$CO_3{}^{-2} + 10H^{+} + 8e^{-} - 3H_2O \leftrightarrow CH_4$	41.071	2.99
$Mg + \ CO_3{}^{-2} \leftrightarrow MgCO_3$	2.981	0.030
$Na^{+} + \ CO_3{}^{-2} \leftrightarrow NaCO_3{}^{-}$	1.268	
$Na^{+} + H^{+} + \ CO_3{}^{-2} \leftrightarrow NaHCO_3$	10.080	
$Eu^{+3} + OH^{-} \leftrightarrow Eu(OH)^{+2}$	6.200	
$Eu^{+3} + 2OH^{-} \leftrightarrow Eu(OH)_2^{+}$	11.600	
$Eu^{+3} + 3OH^{-} \leftrightarrow Eu(OH)_3$	16.800	
$Eu^{+3} + OH^{-} \leftrightarrow Eu(OH)^{+2}$	3.5	0.1
$Eu^{+3} + 2SO_4{}^{-2} \leftrightarrow Eu(SO_4)_2^{-}$	5.2	0.2
$Eu^{+3} + Cl^{-} \leftrightarrow EuCl^{+2}$	0.34	0.05
$Eu^{+3} + 2Cl^{-} \leftrightarrow EuCl_2^{+}$	0.05	
$Eu^{+3} + CO_3^{-2} \leftrightarrow EuCO_3^{+}$	7.900	
$Eu^{+3} + 2CO_3^{-2} \leftrightarrow Eu(CO_3)_2^{-}$	12.900	
$Eu^{+3} + HCO_3^{-} \leftrightarrow EuHCO_3^{+}$	2.1	
$Eu^{+3} + 2HCO_3^{-} + H_2O \leftrightarrow EuH(CO_3)_2^{-2} + 3H^{+}$	-15.2	
$Eu^{+3} + HCO_3^{-} + 2H_2O \leftrightarrow Eu(OH)_2(CO_3)^{-} + 3H^{+}$	-17.8	
$Eu^{+3} + 3HCO_3^{-} \leftrightarrow Eu_2(CO_3)_3 + 3H^{+}$	-5.8	
$Eu^{+3} + CO_3^{-2} + H_2O \leftrightarrow EuOHCO_3 + H^{+}$	-7.8	

The activity coefficient is used to balance the impact of a species with high

concentration to other ions. It is calculated by Specific-ion Interaction Theory (SIT), and the JAEA TDB is used in this model, which contains SIT parameters for a large number of aqueous species. However, the JAEA TDB does not have the Eu element related data, so there are other data from other articles (Tertre E and other, 2006). SIT values from JAEA TDB that uses in the model are shown in the table below:

Table 7:SIT parameters for relevant species in the JATA TDB (Kitamura et al., 2014) and another article (Tertre E and other, 2006)

Species 1	Species 2	Epsilon value	Error
H^{+}	Cl^{-}	0.12	0.01
Mg^{+2}	Cl^{-}	0.19	0.02
Ca^{+2}	Cl^{-}	0.14	0.01
OH^{-}	Na^{+}	0.04	0.01
OH^{-}	K^{+}	0.09	0.01
Cl^{-}	Na^{+}	0.03	0.01
Cl^{-}	K^{+}	0.00	0.01
HSO_4^{-}	Na^{+}	-0.01	0.02
SO_3^{-2}	Na^{+}	-0.08	0.05
SO_4^{-2}	Na^{+}	-0.12	0.06
SO_4^{-2}	K^{+}	-0.06	0.02
$S_2O_3^{-2}$	Na^{+}	-0.08	0.05
Eu^{+3}	Cl^{-}	0.23	0.02
$Eu(OH)^{+2}$	Cl-	-0.04	0.07
$Eu(OH)_2^{+}$	Cl-	-0.27	0.20
$Eu(SO_4)_2^{-}$	Na^{+}	-0.05	0.05

Eu $(CO_3)^+$	Cl-	0.01	0.05
Eu $(CO3)_2$-	Na^+	-0.14	0.06
HCO_3^-	Na^+	0	0.02
HCO_3^-	K^+	-0.06	0.05
CO_3^{-2}	Na^+	-0.08	0.03
CO_3^{-2}	K^+	0.02	0.01

In this PHREEQC model, the data block PHASES define the dissolution reaction in the model, and in this model, it is more expected to describe the precipitation process, which should have greater impact rather than dissolution process. The data is from JAEA TDB database and other articles, which is shown in the table below:

Table 8: The reaction equation and constant for dissolution reaction

Formation reaction	Log K	Error
$CaSO_4 \cdot 2H_2O(gypsum) \leftrightarrow Ca^{+2} + SO_4^{-2} + 2H_2O$	-4.6	0.02
$CaSO_4(anhydrite) \leftrightarrow Ca^{+2} + SO_4^{-2}$	-4.380	
$CaO(s) \leftrightarrow Ca^{+2} + H_2O - 2H^+$	32.700	
$MgO(periclase) \leftrightarrow Mg^{+2} + H_2O - 2H^+$	21.580	
$Ca(cr) \leftrightarrow Ca^{+2} + 2e^-$	96.847	0.184
$CaO(cr) \leftrightarrow Ca^{+2} + H_2O - 2H^+$	32.699	0.244
$Na(cr) \leftrightarrow Na^+ + e^-$	45.892	0.017
$K(cr) \leftrightarrow K^+ + e^-$	49.493	0.020
$S(cr) \leftrightarrow SO_4^{-2} - 4H_2O + 8H^+ + 6e^-$	-35.836	0.075
$Mg(cr) \leftrightarrow Mg^{+2} + 2e^-$	79.778	0.234
$NaCl(cr) \leftrightarrow Na^+ + Cl^-$	1.568	0.037
$Eu(OH)_3(s) \leftrightarrow Eu^{+3} + 3OH^-$	-26.9	0.5

$Eu_2O_3(cubic) \leftrightarrow 2Eu^{+3} + 3H_2O - 6H^+$	52.4	0.01
$Eu_2O_3(monoclinic) \leftrightarrow 2Eu^{+3} + 3H_2O - 6H^+$	54.0	
$Eu_2(CO_3)_3 \cdot 6H_2O(s) \leftrightarrow 2Eu^{+3} + 3CO_3^{-2} + 6H_2O$	-35.0	
$Eu_2(SO_4)^3 \cdot 8H_2O(s) \leftrightarrow 2Eu^{+3} + SO_4^{-2} + 8H_2O$	-10.2	0.02
$EuCl_3 \cdot 6H_2O(s) \leftrightarrow Eu^{+3} + 3Cl^- + 6H_2O$	5.2	0.01
$EuOCl(s) \leftrightarrow Eu^{+3} + H_2O + Cl^- - 2H^+$	15.81	0.01
$Eu(OH)_2Cl(s) \leftrightarrow Eu^{+3} + 2OH^- + Cl^-$	-18.87	0.01
$Eu(OH)_{2.5}Cl_{0.5}(s) \leftrightarrow Eu^{+3} + 2.5OH^- + 0.5Cl^-$	-22.11	0.001

4.2 Surface Definitions

In PHREEQC, the SURFACE data block defines the surface sorption properties of the solid that is being applied in the model. The surface sorption property is defined by the surface density (number per nanometer), the specific surface area (m^2/g) and the total mass of solid (g), and calculated by multiply three properties together. Also, instead of all above, the surface sorption property can be defined by just set the number of sites, in mol, in the 1L solution system. In this model, the MX-80 bentonite is evaluated. As discussed in chapter 2.1, the strong & weak site of sorption model and ionic exchange between bentonite and Eu (III) are need to considered in the model. So, for each solid, one group of strong site properties, one group of ionic exchange site, and two groups of weak site properties is set in the model.

For the property total mass of solid (g), since the total solution volume that been applied in the model is always been 1L, the total mass of solid is determined by liquid/solid ratio of the experiment, and that is, when the L/S ratio is 10mL/10mg, the property total mass of solid (g) should be set as 1 (g). For other two parameters, they are depending on the chemical characteristic of each rock. The property data is initially references from other articles, and

optimized based on experiment data and other article results, and the detail will be discussed in chapter 5. The summarizes of the surface properties of MX-80 bentonite is listed below:

Table 9: Surface properties of solids used in the sorption models

Solid	Site	No. of sites(mol)	Site Capacity (mol/kg)	Grams
MX-80 Bentonite	Strong	1e-6	26.2	1
	Ionic exchange site [Na]	6e-4		1
	Weak 1	1.09e-5		1
	Weak 2	1.09e-5		1

4.3 Surface complex reactions

As mentioned in chapter 2.1, various of sorption happens on the surface site, and with different solid, the surface complexation reactions have different constant coefficients. In this model, it focuses on setting the sorption equations of Acid-Base Equilibria and metal binding, as what it mentioned in chapter 2.1.2, and ionic exchange on solid as mentioned in chapter 2.1.3.

The acid-base equilibria equations are related with the pH value of the solution, which need to be set. The metal binding equations are related with the sorption of the target element Eu (III), which are the values that need to be figured by using experiment data. The function of specific sorption, described in chapter 2.2, are also shown in this figure. The ionic exchange equations are related with the Na ions on bentonite and solution ions (Eu^{3+}, H^{+}, Ca^{2+}, K^{+}, Mg^{2+}, Ba^{2+}, Sr^{2+}), reference the data from yukio Tachi (2014), X. Hurel (2010) and B. Grambow (2006). These equations with different constant coefficients K shown in logarithmic form for each solid and surface site is shown below:

Table 10:Surface complex reaction equations

Surface complexation reaction	site	Constant coefficient logK
$S-OH+H^+ \rightleftharpoons S-OH_2^+$	Strong	4.5
	Weak 1	4.5
	Weak 2	6.0
$S-OH \rightleftharpoons S-O^- + H^+$	Strong	-7.9
	Weak 1	-7.9
	Weak 2	-10.5
$S-OH+Eu^{3+} \rightleftharpoons S-OEu^{2+}+H^+$	Strong	2.2
$S-OH+Eu^{3+}+2H_2O \rightleftharpoons S-OEu(OH)_2+3H^+$	Strong	-15
$X-Na+H^+ \rightleftharpoons X-H+Na^+$	Ionic ex	1.0
$2X-Na+Ca^{2+} \rightleftharpoons X_2-Ca+2Na^+$	Ionic ex	2.7
$X-Na+K^+ \rightleftharpoons X-K+Na^+$	Ionic ex	0.5
$2X-Na+Mg^{2+} \rightleftharpoons X_2-Mg+2Na^+$	Ionic ex	2.4
$2X-Na+Ba^{2+} \rightleftharpoons X_2-Ba+2Na^+$	Ionic ex	0.7
$2X-Na+Sr^{2+} \rightleftharpoons X_2-Sr+2Na^+$	Ionic ex	0.7
$3X-Na+Eu^+ \rightleftharpoons X_3-Eu+3Na^+$	Ionic ex	5

5. Result and analysis

5.1 Detection limit of Eu (III) by ICP-MS

The measurement result for the Eu (III) detection limit test are shown in the table below.

Table 11:Eu(III) measurement in deionized water by ICP-MS

	151 Eu [No Gas]		153 Eu [No Gas]		209 Bi (ISTD) [No Gas]	
Actual concentration [M]	CPS	CPS RSD	CPS	CPS RSD	CPS	CPS RSD
DI Rinse	70.00333	57.7	84.45667	47.8	47862200	1.3
1x10-7	940436.6	0.4	1051499	1.2	46715611	0.1
1x10-8	47381.37	1.3	51984.2	2.6	46991035	0.6
1x10-9	12769	4.6	14493.72	2.6	46426401	1.3
1x10-10	6592.477	1.4	7457.637	2.4	48919507	1.5
1x10-11	368.9067	24.5	416.69	11.9	49653004	1
1x10-12	133.34	2.5	146.6733	17.2	49394848	0.8
1x10-13	101.1167	19.3	125.56	29.6	48514871	1

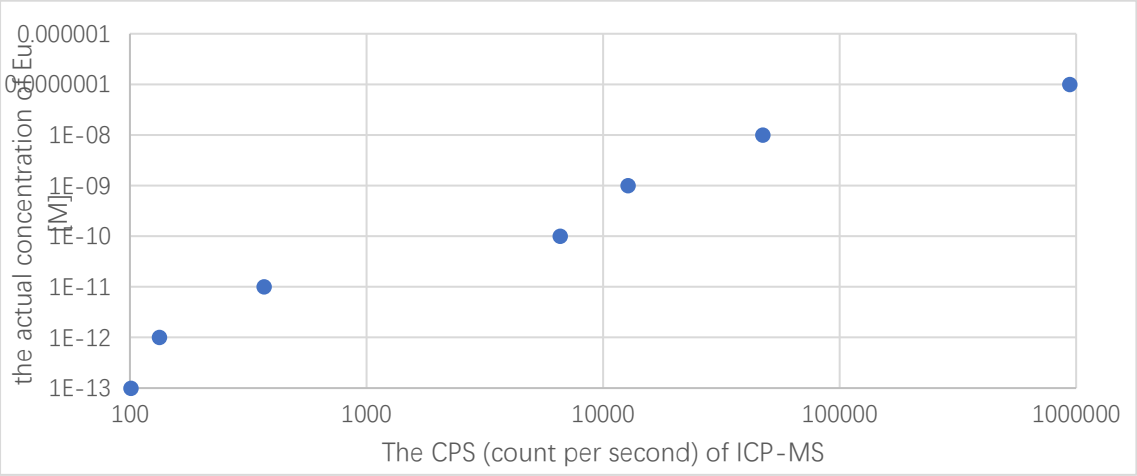

Figure 18: the Eu (III) measurement in deionized water by ICP-MS

In the table, there are two Eu (III) detections. The 151 Eu [No Gas] displace the measurement result based on the element ^{151}Eu, and the 153 Eu [No Gas] displace the measurement result based on the element ^{153}Eu. The corresponding counts per second (CPS) value shows the detection ability of ICP-MS on the target sample, and it can be seen that when the actual concentration of the sample went down, the CPS result also went down. The 209 Bi (ISTD) [No gas] is the background test, the Bi sample is used as the detection of flow rate, and make sure the flow rate is stable. If the flow rate increases, both CPS value of Eu and Bi will increase, and the result of Bi CPS can correct the impact of flow rate on the Eu measurement result.

5.2 Eu (III) solubility

The solubility of Eu (III) in Na-Ca-Cl (Na/Ca ratio 2.7) solutions with ionic strength 0.1M and 6M is shown below.

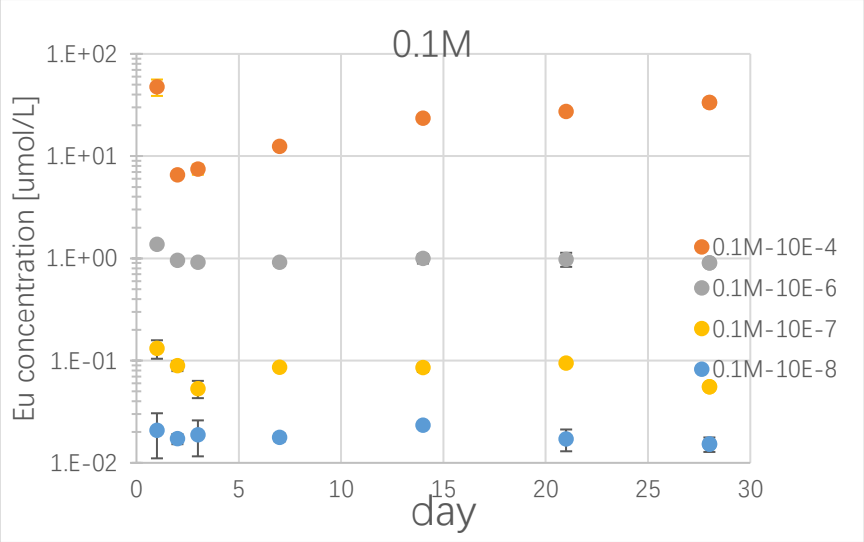

Figure 19: The solubility of Eu (III) in Na-Ca-Cl 0.1M solution

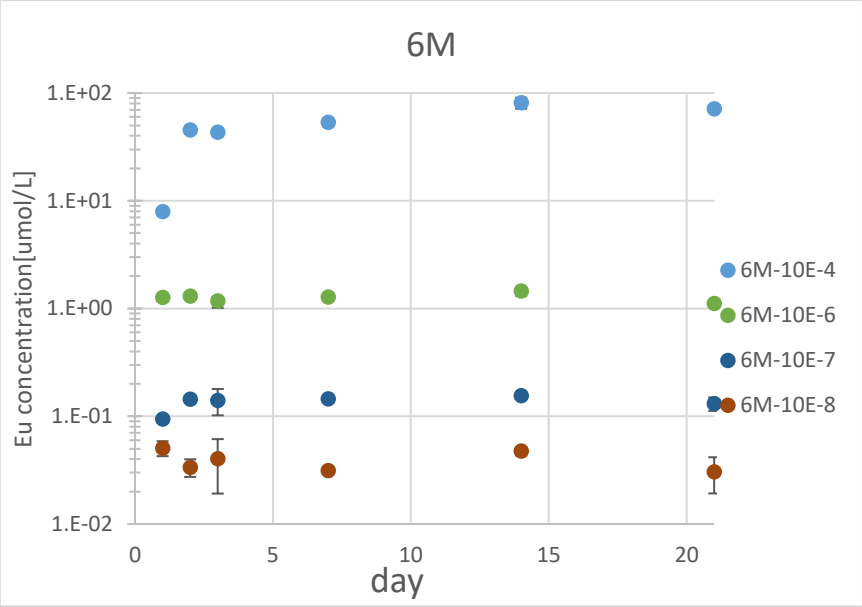

Figure 20: The solubility of Eu (III) in Na-Ca-Cl 6M solution

The concentration of Eu is measured in the 30 days. In Na-Ca-Cl solution with ionic strength 0.1M, the solubility figure shows, when Eu (III) concentration is at 10E-4 M, the detected concentration is much lower than actual concentration, whenever in day 1 and day 28. And, when Eu (III) concentration is at 10E-6M, 10E-7M, the detected concentration is same as the detected concentration, which means the Eu (III) solubility is higher than 10E-6M in the same environment when ionic strength is 0.1M. In Na-Ca-Cl solution with ionic strength 6M, the solubility figure shows, when Eu (III) concentration is at 10E-4 M, the detected concentration is much lower than actual concentration in the first 10 days, which means the solubility of Eu (III) is lower than 10E-4M. And, when Eu (III) concentration is at 10E-6M, 10E-7M, the detected concentration is same as the detected concentration, which means the Eu (III) solubility is higher than 10E-6M in the same environment when ionic strength is 6M.

5.3 Eu (III) sorption kinetics

The results of sorption kinetic experiment are shown in the figure below.

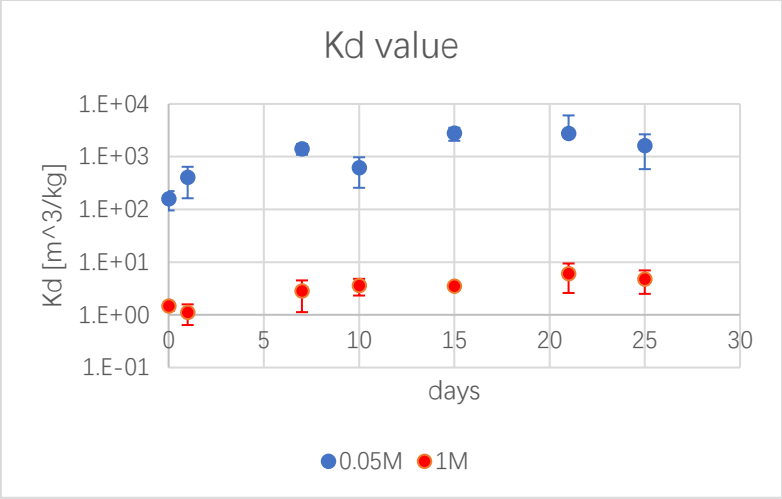

Figure 21: Kinetic experiment for Eu on MX-80 in Ca-Na-Cl solutions

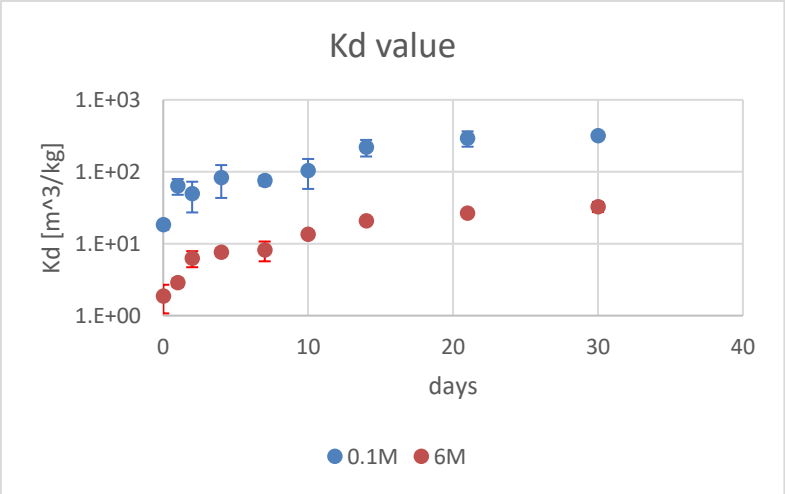

Figure 22: Kinetic experiment for Eu on MX-80 in Na-Ca-Cl solutions

The kinetic experiment in Ca-Na-Cl solutions including ionic strength 0.05M and 1M, within 25 days. For both 0.05M and 1M, the Kd of Eu sorption is continue rising from day 1 to day 10, and becomes stable in day 15. The kinetic experiment in Na-Ca-Cl solutions including ionic strength 0.1M and 6M, within 30 days. For both 0.05M and 1M, the Kd of Eu sorption is continue rising from day 0 to day 21, and becomes stable from day 21. In both cases, which includes all possible situations in the experiment, shows the Eu (III) sorption kinetics, and 30 days is selected to be a time period that can make Eu (III) sorption stable onto the MX-80 bentonite in the experiment environment.

5.4 pH and ionic strength dependence of Eu (III) sorption

The pH dependence of Eu (III) sorption on MX-80 in Na-Ca-Cl (Na/Ca ratio 2.7) solution with ionic strength from 0.1M to 6M.

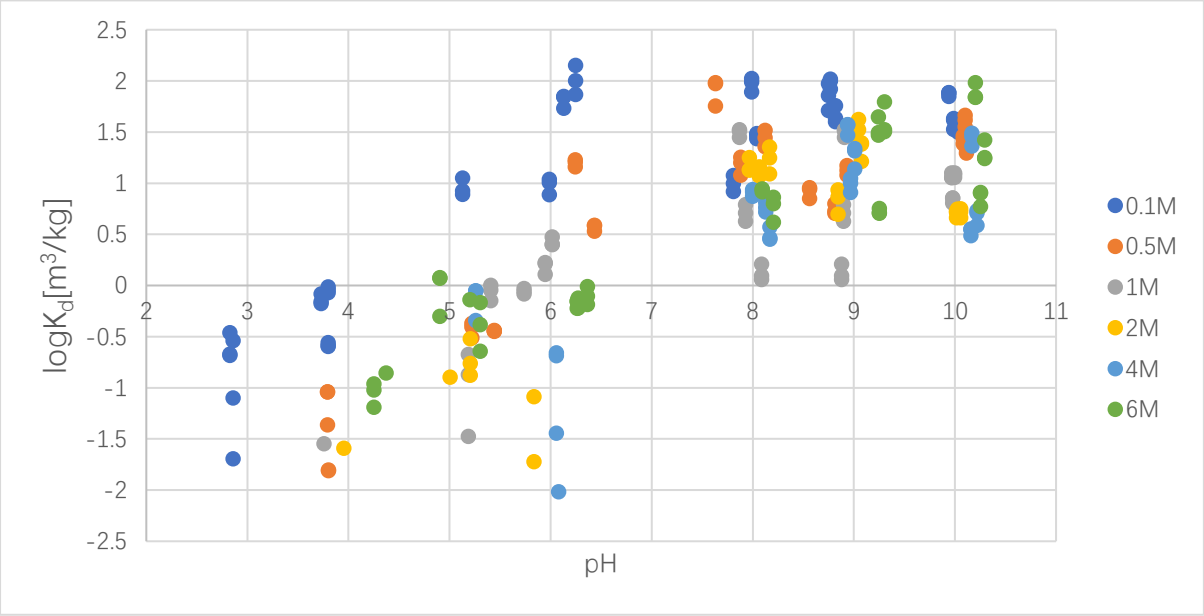

Figure 23: pH dependence of Eu (III) sorption on MX-80 in Ionic strength between 0.1M and 6M

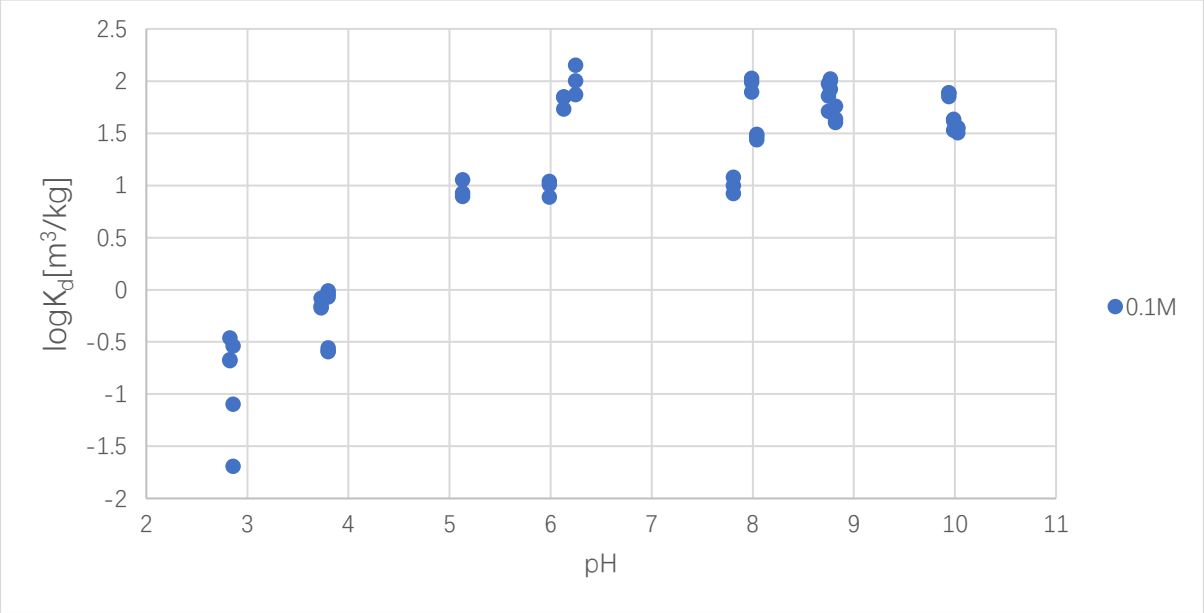

Figure 24: pH dependence of Eu (III) sorption on MX-80 in Ionic strength 0.1M

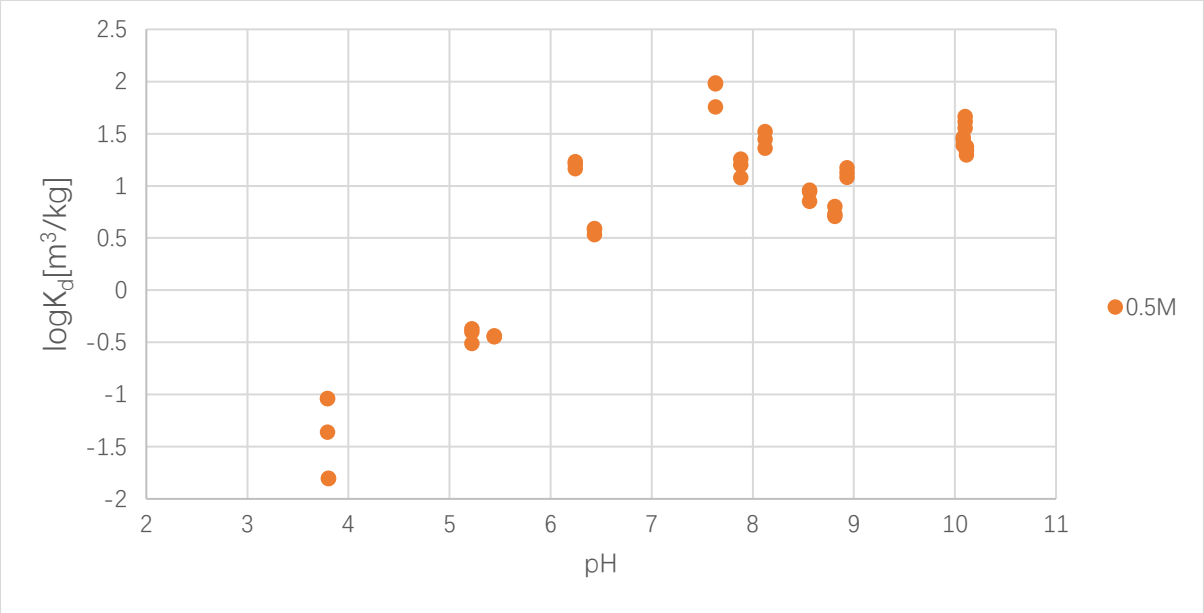

Figure 25:pH dependence of Eu (III) sorption on MX-80 in Ionic strength 0.5M

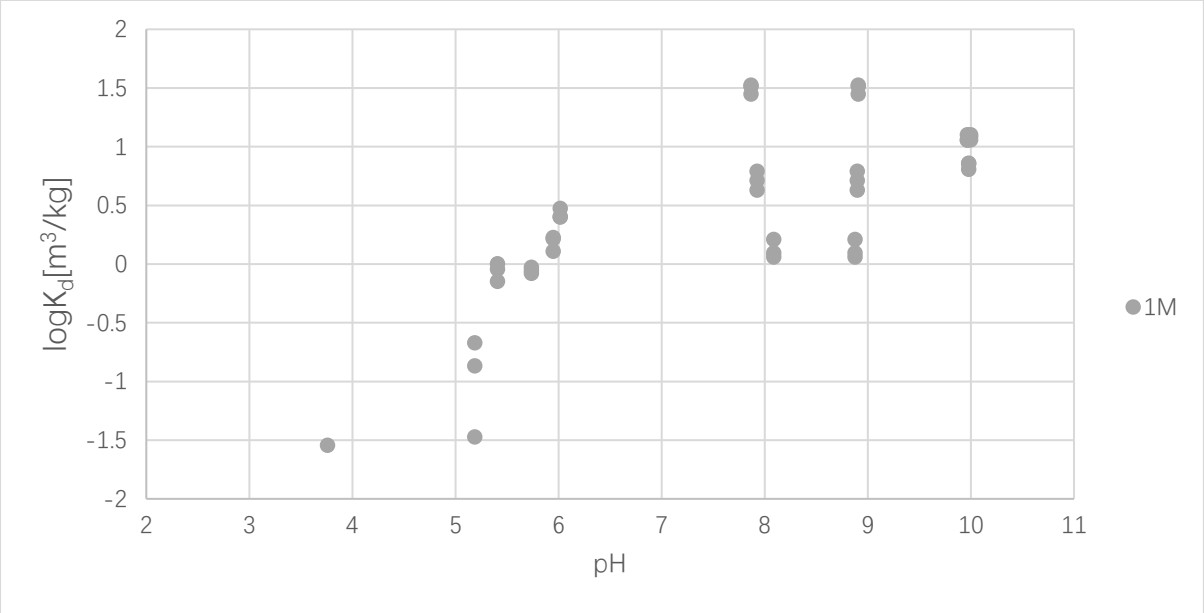

Figure 26:pH dependence of Eu (III) sorption on MX-80 in Ionic strength 1M

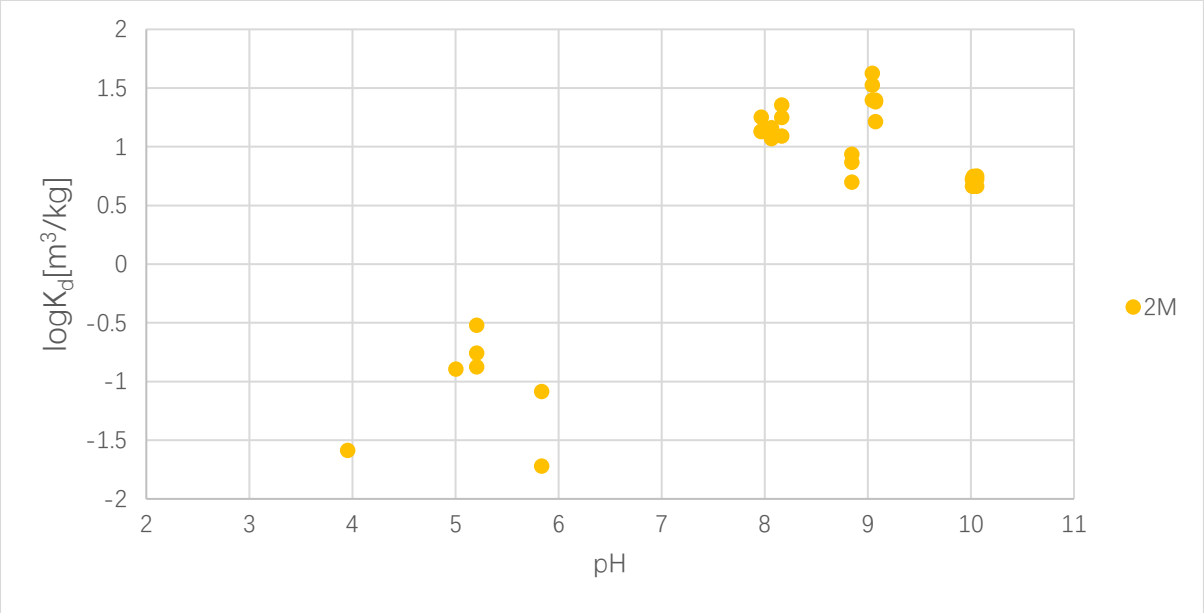

Figure 27: pH dependence of Eu (III) sorption on MX-80 in Ionic strength 2M

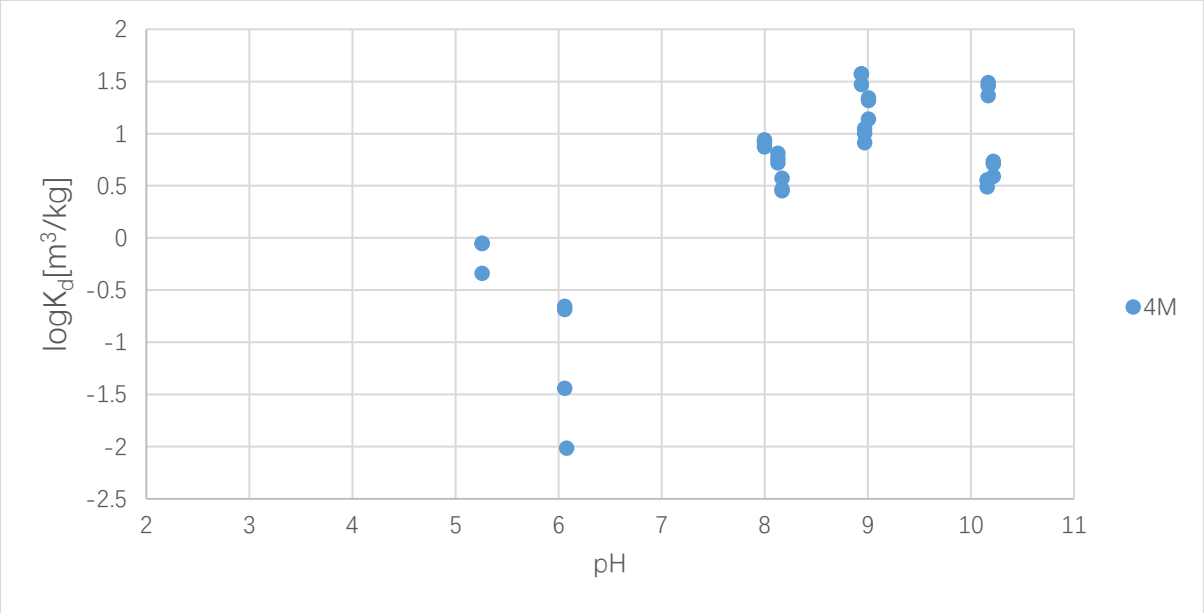

Figure 28: pH dependence of Eu (III) sorption on MX-80 in Ionic strength 4M

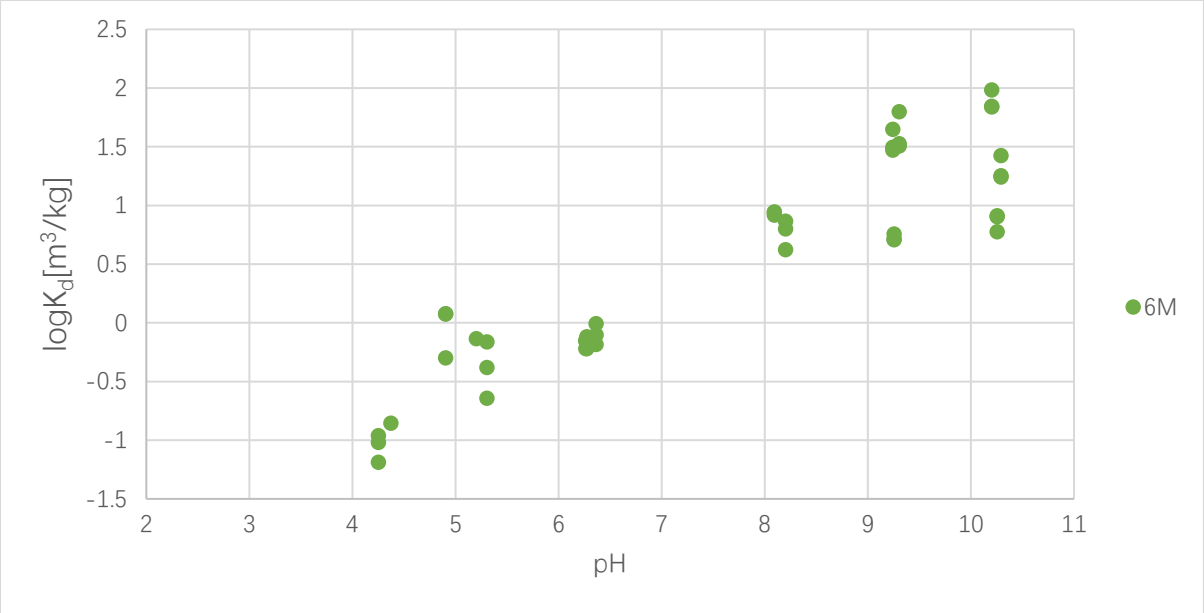

Figure 29: pH dependence of Eu (III) sorption on MX-80 in Ionic strength 6M

There are clear trends can be observed in all experiment about pH and ionic strength dependence. For pH dependence, the sorption is not significance in pH at 3, and start to be measured at pH at 4. Then, from pH 4 to 6 at 0.1M, pH 4 to 8 at 0.5M and 1M. pH 4 to 9 at 2M and 4M, and pH 4 to 10 at 6M, the sorption Kd value is rapidly increasing. After that the pH continues increases, the Kd value, which is the sorption behavior, becomes stable and even slight decreasing, and that happens when pH 6 to 10 at 0.1M, pH 8 to 10 at 0.5M and 1M, pH 9 to 10 at 2M and 4M. The ionic strength dependence is also shown in the figure. It can be seen that when pH is at 4 to 9, which means most of the possible environments, the higher ionic strength has lower K_d value, which means lower K_d sorption behavior. When pH reaches a very high level, the sorption behavior for different ionic strength seems converge, and it can be observed from high pH range (9 to 10) in different ionic strength samples, which the Kd value becomes similar.

5.5 PHREEQC Surface complexation modelling

The PHREEQC model verification for Eu (III) surface complexation has been completed. In the PHREEQC model, the solubility and speciation of the europium in

particular solution (SR-270-PW, CR-0, CR-10, CR-10NF, Na-Ca-Cl experiment solutions, Ca-Na-Cl experiment solutions) can be calculated. And, it has the ability to describe the Eu (III) sorption behavior on MX-80 in different aspects: the number of surface site speciation, the number of surface complex and ionic exchange speciation, and the sorption behavior expressed by Kd. They all present with pH related, and some of the results are posted below.

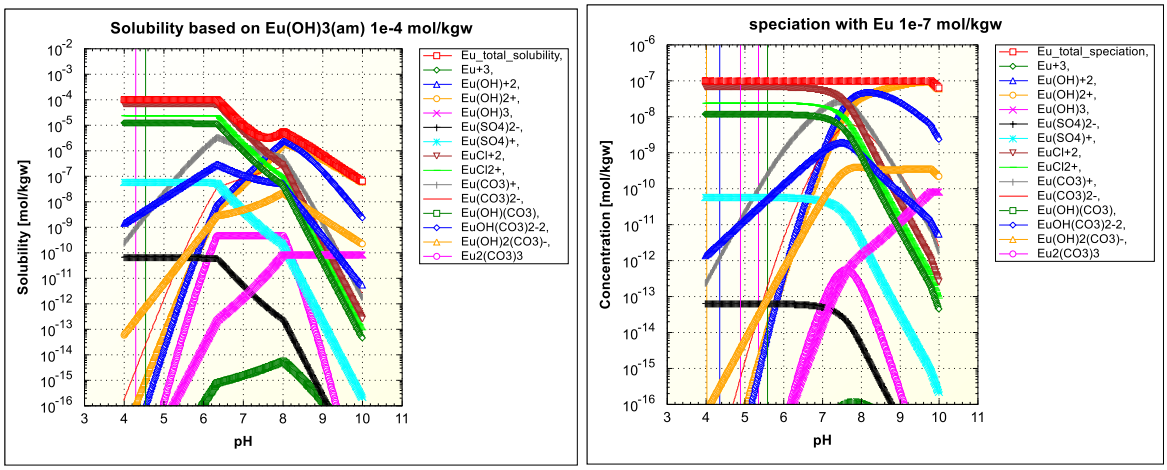

Figure 30: Solubility and speciation of Eu (III) in SR-270-RW solution

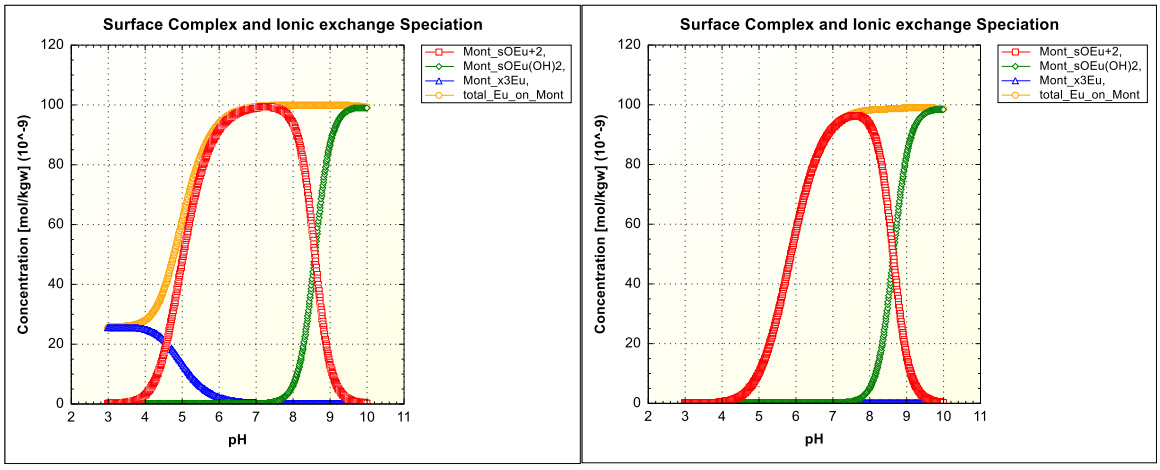

Figure 31:Surface complex and ionic strength speciation in ionic strength 0.1M and 4M

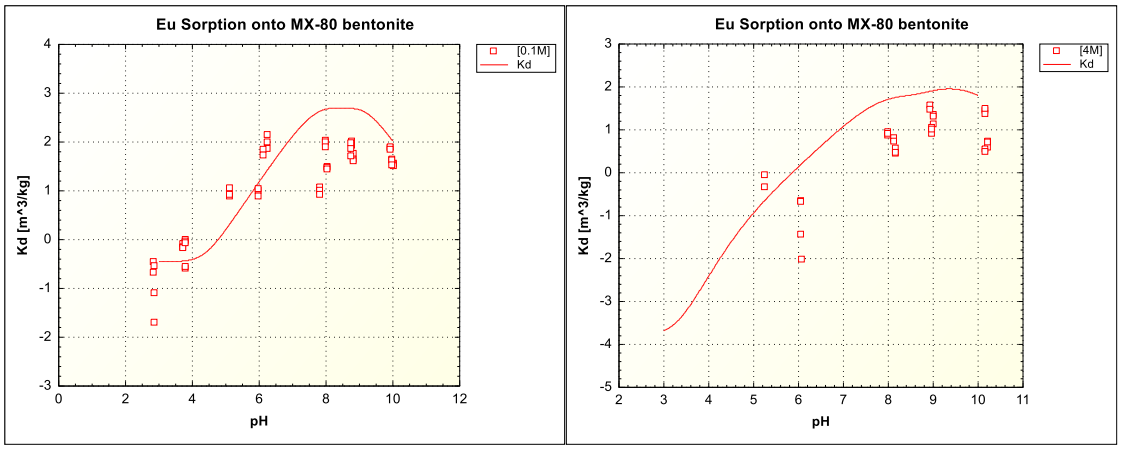

Figure 32:Sorption behavior K_d with pH related when ionic strength 0.1M and 4M, and compare with experiment results

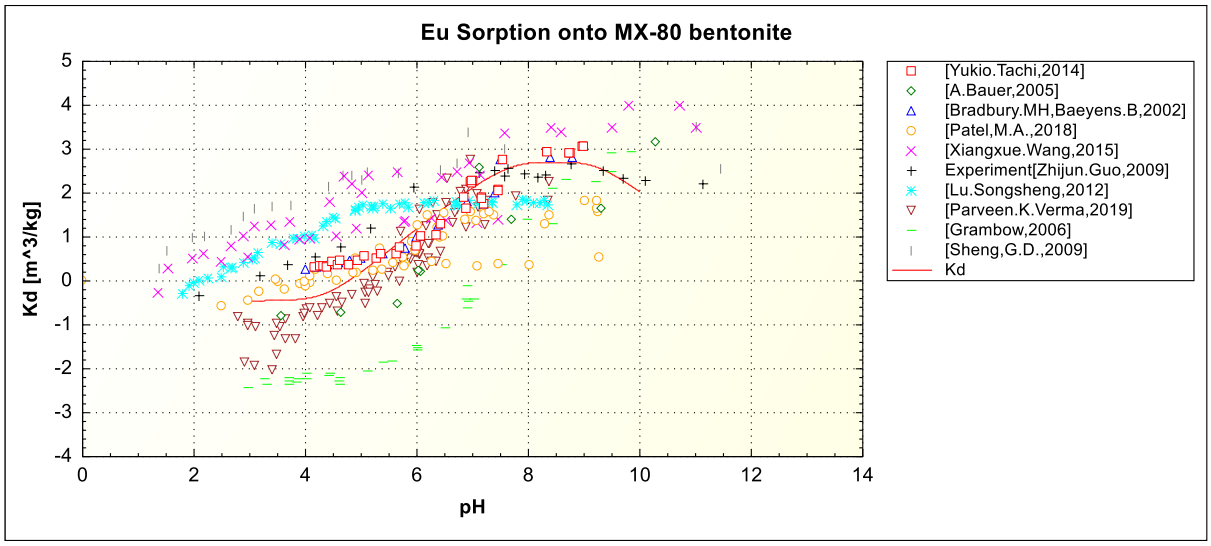

Figure 33: Sorption behavior K_d with pH related, and compared with other research results

6. Discussion

6.1 Detection limit of Eu (III) by ICP-MS

From the result that posted in chapter 5.1, it is found that the detection limit for Eu by ICP-MS is approximately 1E-12 M, when the sensitivity of ICP-MS is at its normal situation. So, it is reliable to pre-set the detection limit of ICP-MS when deciding the whole experiment process to be 5E-12M (five times as the detection limit result in this experiment).

The value of detection limit is critical for deciding the initial concentration of Eu and other related parameters in the kinetic sorption experiment, and the rest of the experiment. The initial concentration of Eu in kinetic sorption experiment is set to be 1E-6M, and adjusted to 1E-7M in the pH & ionic strength depending experiment. The solubility experiment will also determine the if the solubility is higher or lower than 1E-6M and 1E-7M in the experimental environment. The solution in each sample is determined to be 10 ml, the MX-80 bentonite in each sample in each sample in kinetic sorption experiment is determined to be 20 mg, and adjusted to 10 mg in the pH & ionic strength depending experiment.

6.2 Eu (III) solubility

The solubility experiment is to test the influence of ionic strength of solution onto the solubility of Eu (III), and determine the initial concentration of the rest experiments. For the solution Eu initial concentration 1E-4M with ionic strength 0.1M and 6M, the concentration of Eu (III) are drastic changes for the samples, which proves the solubility is significantly lower than 1E-4M in all experimental conditions. For initial concentration 1E-6M, 1E-7M and 1E-8M, with both ionic strength 0.1M and 6M, the measured concentration during day 1 to day 28 keeps stable, and that means the solubility of Eu in experiment conditions (ionic strength 0.1M ~ 6M) is higher than 1E-6M, and that proves the reliability of the experiment.

6.3 Eu (III) sorption kinetics

The sorption kinetics experiment shows that sorption speed of Eu on MX-80 bentonite in Na-Ca-Cl and Ca-Na-Cl experiment solution on its maximum and minimum experiment ionic strength condition. In Na-Ca-Cl solutions, the sorption is significantly very high on the day 1, and slowly increased between day 1 and day 15, and becomes constant after day 15. In Ca-Na-Cl solutions, the sorption is slowly increased from day 0 to day 14, and becomes constant after day 21. In both solutions, the difference of ionic strength is not

influencing the sorption kinetics, and only influences the sorption abilities, which will discuss in the chapter 6.4.

For the future experiments, it is determined that sorption equilibrium has been reached after 21 days in all experiment conditions. For ensure the sorption equilibrium will be certainly reached, the equilibrium time for the next experiments was chose to be 30 days. Furthermore, the data obtained in less 14 days in similar experiment operation and conditions could be seen as unreliable.

6.4 The pH and ionic strength dependence of Eu (III) sorption

The chapter 5.4 shows the pH dependence of Eu (III) sorption on MX-80 in Na-Ca-Cl (Na/Ca ratio 2.7) solution with ionic strength from 0.1M to 6M, and the data shows the clear pH and ionic strength dependence of Eu sorption onto MX-80 bentonite.

For ionic strength is 0.1M, when pH is at 4, the sorption starts to increase, rapidly increases when pH is between 4 to 6, and keeps in a high constant when pH is higher than 8. When the pH is 9 and 10, there is small drop for the sorption but not obvious. The similar things happen in other samples with different ionic strength, and in higher ionic strength, the sorption behavior based on pH is more delayed, which means the sorption K_d value with the lower pH in lower ionic strength environment correspond with the K_d value with higher pH in higher ionic strength environment.

According to the TRLFS and XAFS reference in chapter 1.1.2, in low pH condition, the Eu^{3+} are the main species of Eu (III) in the solution; and in high pH condition, the inner-sphere complex is formed and becomes the main species of Eu. Based on theory in chapter 2, this phenomenon can be explained. Since the initial Eu concentration has been limited into a very low level (1E-7M), the specifical sorption becomes the main sorption behavior during

the experiment process, and two main kinds of specific sorption are happening during the process:

$$S-OH+Eu^{3+} \rightleftharpoons S-OEu^{2+}+H^{+} \quad [\log k = 2.2]$$

$$S-OH+Eu^{3+}+2H_2O \rightleftharpoons S-OEu(OH)_2+3H^{+} \quad [\log k = -15]$$

The equilibrium constant is determined by applying the 2SPNE SC/CE sorption theory onto experiment situation by PHREEQC surface complexation modelling, shown in chapter 5.5.

When the pH is at very low value, which means the H^+ concentration is very high, and that will make both specific sorption rarely to happen. When the pH reaches 4, the concentration of H^+ decreases, that makes the balances moves towards the right side of equation, especially the first one, and sorption product $S-OEu^{2+}$is encouraged to produced. When the pH reaches 8, the concentration of OH^- has increases into a significant level, cooperate with Eu^{3+}, the concentration of Eu^{3+} is reduced and lead the balances tendency to the left. But at the same time, the higher rises of pH also deeper decrease the concentration of H^+, and $S-OEu(OH)_2$ is encouraged to produced. During this stage, the sorption of Eu is maintaining in a high level, until the pH rises too high, and OH^- in the solution cooperate with more Eu^{3+} in the solution, and decreases the sorption behavior of Eu sorption onto bentonite.

The ionic strength dependence is also proving to be available. When pH is at low level, from pH 4 to pH 6, the samples with higher ionic strength have much lower Eu sorption behavior. When pH is at high level, from pH 8 to 10, the samples with higher ionic strength have not obvious lower Eu sorption behavior. Based on the theory in chapter 2, the two main kind of specific sorption are shown:

$S-OH+Eu^{3+} \rightleftharpoons S-OEu^{2+}+H^{+}$ [log k = 2.2]

$S-OH+Eu^{3+}+2H_2O \rightleftharpoons S-OEu(OH)_2+3H^{+}$ [log k = -15]

The high ionic strength reduces the concentration of Eu^{3+}, and makes both specific sorption equation balance shift to the left. When the pH is high, the Eu^{3+} is also reduces by high concentration of OH^{-}, and make the ionic strength dependence insignificant.

6.5 PHREEQC Surface complexation modelling

The 2SPNE SC/CE theory is applied by using PHREEQC modelling, to simulating the sorption process, and successfully reproduced the experiment data of Eu (III) sorption on MX-80 bentonite in all pH range with both highest and lowest ionic strength, and fits the data that collected from other reliable research with similar experiment conditions. Therefore, it is determined that the model has working usefully and would produce reliable results.

The solubility and speciation of the europium in particular solution (SR-270-PW, CR-0, CR-10, CR-10NF, Na-Ca-Cl experiment solutions, Ca-Na-Cl experiment solutions) can be calculated, and has been confirmed to be reliable and reasonable.

The main application for PHREEQC is on simulating the Eu sorption onto MX-80 bentonite. The chapter 5.5 shows the surface complex and ionic exchange speciation results, and sorption complexation reactions result compared it with data from this experiment, and the sorption result from other reliable researches. By fitting the experiment result, the equilibrium constants for two main surface complex reactions can be determined as 2.2 and -15, as chapter 6.4 shows. The modelling result is used in analysing the sorption process in chapter 6.4, helps the researchers to theoretically simulating the sorption process.

The last figure in chapter 5.5 shows, the model production result is compared with the data from 10 different reliable researches, from Yukio, Tachi (2014), A. Bauer (2005),

Bradbury. MH. Baeyens. B, (2002), Patel. M. A, (2018), Xiangxue Wang (2015), Zhijun Guo (2009). Lu, Songsheng (2012), Parveen. K. Verma (2019), Grambow (2006), and Sheng, G. D (2009). The comparation result shows the modelling result have the similar tendency and sorption ability with the result from researches in similar experiment conditions, and confirmed the reliability of the modelling, the experiment result, and the sorption theory that developed in this experiment.

7. Conclusions

The study of the sorption of Eu in low concentration on MX-80 bentonite under highly saline, reducing conditions and the application of 2SPNE SC/CE sorption model to simulate sorption behavior is successfully finished. And, during the process, some other achievements have been made.

The detection limit of Eu by ICP-MS is determined to be approximately 1E-12M. Based on this, and under the setting of maintaining the low Eu concentration, the detection limit allows K_d values of up to 999 m3/kg to be measured.

The solubility limit of Eu in Na-Ca-Cl solutions with both ionic strength 0.1M and 6M has determined to be higher than 1E-6M. So, the initial concentration of Eu at 1E-6M in kinetic sorption experiment and 1E-7M in pH & ionic strength dependence sorption experiment is proved to be lower than solubility limit and is accepted to use.

Sorption kinetics for Eu (III) has been successfully measured for MX-80 bentonite in Ca-Na-Cl solution with ionic strength 0.05M and 1M, and Na-Ca-Cl solution with ionic strength 0.1M and 6M. It was found that the sorption in Ca-Na-Cl solution reaches equilibrium in 15 days, and in Na-Ca-cl solutions reaches equilibrium in 21 days, in all ionic strengths. For consistency, 30 days is selected as the placement time for the subsequent experiment

Sorption pH & ionic strength dependence experiments illustrated that MX-80 bentonite have higher sorption on Eu for higher pH values and lower ionic strength. In more detail, in most cases when ionic strength is not too high (0.1M to 4M), in the range of pH at 4 to 9, the higher pH prompted the improvement of sorption ability. But, when pH is out of range and getting too high, the higher pH prompted the decreases of sorption ability. And for

the dependence of ionic strength, in general, in rise of ionic strength causes the decreases of sorption behavior of MX-80 bentonite, and this relation is weakening when the pH rises.

A PHERRQC model is developed to simulate the sorption of Eu (III) onto MX-80 bentonite to investigate the sorption mechanisms. This model successfully determined the solubility and speciation of Eu (III) in different kind of solutions (SR-270-PW, CR-0, CR-10, CR-10NF, Na-Ca-Cl experiment solutions, Ca-Na-Cl experiment solutions), and successfully reproduced sorption results for Eu (III) experiment result and data from other research articles. Therefore, the reliability of the model is proved.

8. Bibliography

A. Bauer, T. Rabung, F. Claret, T. Schfer, G. Buckau, T. Fanghnel, (2005). *Influence of temperature on sorption of europium onto smectite: The role of organic contaminants, Applied Clay Science,* Volume 30, Issue 1, 2005, Pages 1-10, ISSN 0169-1317,

Alexander Cruden, Andreas Gautschi, Anders Strom, Michael Stephens and Peter K Kalser, (2020). *2020 Report of the NWMO Adaptive Phased Management Geoscientific Review Group (GRG).* NWMO. December 202

Allison, J.D., Brown, D.S., and Novo-Gradac, K.J. (1991), *MINTEQA2/PRODEFA2—A geochemical assessment model for environmental systems—Version 3.0 user's manual*: Athens, Georgia, Environmental Research Laboratory, Office of Research and Development, U.S. Environmental Protection Agency, 106 p.

Ball, J.W., and Nordstrom, D.K., 1991, *WATEQ4F—User's manual with revised thermodynamic data base and test cases for calculating speciation of major, trace and redox elements in natural waters*: U.S. Geological Survey Open-File Report 90–129, 185 p.

B. Grambow, M. Fattahi, G. Montavon, C. Moisan, and E. Giffaut. (2006). *Sorption of Cs, Ni, Pb, Eu(III), Am(III), Cm, Ac(III), Tc(IV), Th, Zr, and U(IV) on MX 80 bentonite: An experimental approach to assess model uncertainty,* Radiochimica Acta, vol. 94, no. 9–11, pp. 627–636,

Bradbury, M.H., Baeyens, B., (2002). *Sorption of Eu on Na and Camontmorillonite: Experimental investigations and modeling with cation exchange and surface complexation*. Geochim. Cosmochim. Acta 66, 2325–2334.

Bradbury MH, Baeyens B (2002) Geochim Cosmochim Acta 66:2325–2334

Bradbury, M. H., & Baeyens, B. (2011). *Physico-chemical characterisation data and sorption measurements of Cs, Ni, Eu, Th, U, Cl, I and Se on MX-80 bentonite*. (PSI Bericht, Report No.: 11-05). Paul Scherrer Institut.

C. Hurel and N. Marmier, (2010). "Sorption of europium on a MX-80 bentonite sample: experimental and modelling results," Journal of Radioanalytical and Nuclear Chemistry, vol. 284, no. 1, pp. 225–230.

Cyrille Alliot, Lionel Bion, Florence Mercier, Pierre Toulhoat. (2006). *Effect of aqueous acetic, oxalic, and carbonic acids on the adsorption of europium (III) onto r-alumina, Journal of Colloid and Interface Science,* Volume 298, Issue 2, 2006, Pages 573-581, ISSN 0021-9797.

Davies, C. W. (1962*). Ion Association*. Butterwoths Pub., Washington, DC.

Debye, P. and Huckel, E. (1923). *Zur Theorie der Elektrolyte. I. Gefrierpunktserniedrigung und verwandte Erscheinungen [The theory of electrolytes. I. Lowering of freezing point*

and related phenomena]. Physikalische Zeitschrift, 24, 185{206.

Endo, M. & Takeda, T. & Kim, Yong & Koshiba, K. & Ishii, K. (2001). *High Power Electric Double Layer Capacitor (EDLC's);* from Operating Principle to Pore Size Control in Advanced Activated Carbons. Carbon letters. 1.

Eric Simoni. (2002). *Radionuclides retention: from macroscopic to microscopic*, Comptes Rendus Physique, Volume 3, Issues 7–8, 2002, Pages 987-997, ISSN 1631-0705,

E. Tertre. G. Berger. E. Simoni, S. Castet, E. Giffaut, M. Loubet, and H. Catalette. (2006). *Europium retention onto clay minerals from 25 to 150 ºC: Experimental measurements, spectroscopic features and sorption modelling*. ScienceDirect.

G. D. Sheng, D. D. Shao, Q. H. Fan, D. Xu, Y. X. Chen, and X. K. Wang. (2009). *Effect of pH and ionic strength on sorption of Eu (III) to MX-80 bentonite: batch and XAFS study*. Radiochimica Acta International journal for chemical aspects of nuclear science and technology, vol. 97, no. 11, pp. 621–630, Nov. 2009.

Grambow, Bernd, Fattahi, Massoud, Montavon, Gilles, Moisan, C. and Giffaut, E. (2006). *Sorption of Cs, Ni, Pb, Eu(III), Am(III), Cm, Ac(III), Tc(IV), Th, Zr, and U(IV) on MX 80 bentonite: An experimental approach to assess model uncertainty.* Radiochimica Acta, vol. 94, no. 9-11, 2006, pp. 627-636.

Grenthe, I. and Plyasunov, A. (1997). *On the use of semiempirical electrolyte theories for modeling of solution chemical data.* Pure and Applied Chemistry, 69(5), 951{ 958.

Grenthe, Ingmar, Plyasunov, A.V., and Spahiu, Kastriot, (1997), *Estimations of medium effects on thermodynamic data, in Grenthe, Ingmar, and Puigdomenech, Ignasi, eds., Modelling in aquatic chemistry, chap. IX*: Paris, OECD Nuclear Energy Agency, p. 325–426.

J. Chen, M. Behazin, J. Binns, K. Birch, A. Blyth, A. Boyer, S. Briggs, J. Freire-Canosa, G. Cheema, R. Crowe, D. Doyle, J. Giallonardo, M. Gobien, R. Guo, M. Hobbs, M. Ion, J. Jacyk, H. Kasani, P. Keech, E. Kremer, C. Lawrence, A. Lee, H. Leung, K. Liberda, T. Liyanage, C. Medri, M. Mielcarek, L. Kennell-Morrison, A. Murchison, N. Naserifard, A. Parmenter, M. Sanchez-Rico Castejon, U. Stahmer, Y. Sui, E. Sykes, M. Sykes, T. Yang, X. Zhang. (2020). *Technical Program for Long Term Management of Canada's Used Nuclear Fuel – Annual Report 2019*. Nuclear Waste Management Organization.

H. Moll, Th. Stumpf, M. Merroun, A. Rossberg, S. Selenska-Pobell, and G. Bernhard (2004). *Time-Resolved Laser Fluorescence Spectroscopy Study on the Interaction of Curium (III) with Desulfovibrio äspöensis DSM 10631T*. Environmental Science & Technology **2004** 38 (5), 1455-1459

H. Ramebäck, M. Skälberg, U. B. Eklund, L. Kjellberg, and L. Werme, (1998). *Mobility of U, Np, Pu, Am and Cm from Spent Nuclear Fuel into Bentonite Clay,* Radiochimica Acta, vol. 82, no. s1, pp. 167–172, Dec. 1998.

J. Hu et al. (2010). *Sorption of Eu(III) on GMZ bentonite in the absence/presence of humic acid studied by batch and XAFS techniques*, Science China Chemistry, vol. 53, no. 6, pp. 1420–1428, Jun. 2010.

Jinchuan Xie, Jiachun Lu, Jianfeng Lin, Xiaohua Zhou, Mei Li, Guoqing Zhou, Jihong Zhang, (2013). *The dynamic role of natural colloids in enhancing plutonium transport through porous medi*a. Chemical Geology, Volumes 360–361, 2013, Pages 134-141, ISSN 0009-2541,

Kafumbila, K. (2020). *Cobalt precipitation with lime*: Solubility curve. 10.13140/RG.2.2.16816.38409.

Kersting, A., Efurd, D., Finnegan, D. et al. (1999). *Migration of plutonium in ground water at the Nevada Test Site*. Nature 397, 56–59 (1999).

Kitamura, A., Doi, R., & Yoshida, Y. (2014). *Update of JAEA-TDB: Update of Thermodynamic Data for Palladium and Tin, Refinement of Thermodynamic Data for Protactinium, and Preparation of PHREEQC Database for Use of the Brønsted- Guggenheim-Scatchard Model.* Japan Atomic Energy Agency, JAEA-Data/Code 2014-009.

Kowal-Fouchard, A., (2002). *Etude des me´canismes de re´tention des ions U(IV) et Eu(III) sur les argiles: influence des silicates*. Ph.D. Thesis, Universite´ Paris Sud, France, 330p.

Lotfollah Karimzadeh, Holger Lippold, Madlen Stockmann, Cornelius Fischer (2020), *Effect of DTPA on europium sorption onto quartz - Batch sorption experiments and surface complexation modeling*, Chemosphere, Volume 239, 2020, 124771, ISSN 0045-6535,

Lu Songsheng, Xu Hua, Wang Mingming, Song Xiaoping and Liu Qiong. (2012). *Sorption of Eu(III) onto Gaomiaozi bentonite by batch technique as a function of pH, ionic strength, and humic acid.* J Radioanal Nucl Chem (2012) 292:889–895. DOI 10.1007/s10967-011-1532-x.

Madhuri A Patel, Aishwarya Soumitra Kar, Vaibhavi V Raut, B.S. Tomar, (2021). *Probing and understanding interaction of Eu(III) with γ- alumina in presenceof malonic acid, Journal of Environmental Sciences*, Volume 100, 2021, Pages 181-192, ISSN 1001-0742,

Miguel A. Ruiz-Fresneda, Margarita Lopez-Fernandez, Marcos F. Martinez-Moreno, Andrea Cherkouk, Yon Ju-Nam, Jesus J. Ojeda, Henry Moll, and Mohamed L. Merroun. (2020). *Molecular Binding of EuIII/CmIII by Stenotrophomonas bentonitica and Its Impact on the Safety of Future Geodisposal of Radioactive Waste*. Environmental Science & Technology 2020 54 (23), 15180-15190

M. H. Bradbury and B. Baeyens, (2005). *Modelling the sorption of Mn(II), Co(II), Ni(II), Zn(II), Cd(II), Eu(III), Am(III), Sn(IV), Th(IV), Np(V) and U(VI) on montmorillonite: Linear free energy relationships and estimates of surface binding constants for some selected heavy metals and actinides,* Geochimica et Cosmochimica Acta, vol. 69, no. 4, pp. 875–892, Feb. 2005.

M. J. Polinski et al. (2014) *Chirality and Polarity in the f-Block Borates M4[B16O26(OH)4(H2O)3Cl4] (M=Sm, Eu, Gd, Pu, Am, Cm, and Cf),* Chemistry – A

European Journal, vol. 20, no. 32, pp. 9892–9896.

M. Marques Fernandes, A.C. Scheinost, B. Baeyens. (2016). *Sorption of trivalent lanthanides and actinides onto montmorillonite: Macroscopic, thermodynamic and structural evidence for ternary hydroxo and carbonato surface complexes on multiple sorption sites*, Water Research, Volume 99, 2016, Pages 74-82, ISSN 0043-1354,

Neck, V., Müller, R., Bouby, M., Altmaier, M., Rothe, J., Denecke, M., & Kim, J. (2002). Solubility of amorphous Th(IV) hydroxide – application of LIBD to determine the solubility product and EXAFS for aqueous speciation. Radiochimica Acta, 90, 485 - 494.

Parkhurst, D.L., Thorstenson, D.C., and Plummer, L.N., (1990), *PHREEQE—A computer program for geochemical calculations*: U.S. Geological Survey Water-Resources Investigations Report 80–96, 195 p. (Revised and reprinted August, 1990.

Parveen. Kumar. Verma and Prasanta Kumar Mohapatra. (2016). *Effect of different complexing ligands on europium uptake from aqueous phase by kaolinite: batch sorption and fluorescence studies*. Radiochemistry Division, Bhabha Atomic Research Centre, Mumbai-400 085, India

Parveen K. Verma, Anna S. Semenkova, Victoria V. Krupskaya, Sergey V. Zakusin, Prasanta K. Mohapatra, Anna Yu. Romanchuk, Stepan N. Kalmykov, (2019). *Eu(III) sorption onto various montmorillonites: Experiments and modeling*, *Applied Clay Science*, Volume 175, 2019, Pages 22-29, ISSN 0169-1317,

Patel, M.A., Kar, A.S., Kumar, S. et al. (2018). *Correction to: Effect of phosphate on sorption of Eu(III) by montmorillonite*. J Radioanal Nucl Chem 317, 641 (2018).

Patel, Xiangxue Wang, Yubing Sun, Ahemd Alsaedi, asawar Hayat, Xiangke Wang. (2015). *Interaction mechanism of Eu(III) with MX-80 bentonite studied by batch*. Chemical Engineering Journal 264 (2015) 570–576

Pengyuan Gao, Daming Zhang, Qiang Jin, Zongyuan Chen, Dongqi Wang, Zhijun Guo, Wangsuo Wu. (2021) *Multi-scale study of Am(III) adsorption on Gaomiaozi bentonite: Combining experiments, modeling and DFT calculations*, Chemical Geology, Volume 581, 2021, 120414, ISSN 0009-2541,

Peter Vilks and Tammy Yang (2018*). Sorption of Selected Radionuclides on Sedimentary Rocks in Saline Conditions – Updated Sorption Values.* Nuclear Waste Management Organization

Payne, Timothy & Brendler, Vinzenz & Ochs, M. & Baeyens, Bart & Brown, P.L. & Davis, James & Ekberg, Christian & Kulik, Dmitrii & Lützenkirchen, Johannes & Missana, Tiziana & Tachi, Yukio & Van Loon, Luc & Altmann, Scott. (2013). *Guidelines for thermodynamic sorption modelling in the context of radioactive waste disposal. Environmental Modelling & Software*. 42. 143-156. 10.1016/j.envsoft.2013.01.002.

Pitzer, K.S. (1973). *Thermodynamics of electrolytes—1. Theoretical basis and general equations*: Journal of Physical Chemistry, v. 77, no. 2, p. 268–277.

Plummer, L.N., Parkhurst, D.L., Fleming, G.W., and Dunkle, S.A. (1988). *A computer program incorporating Pitzer's equations for calculation of geochemical reactions in brines*: U.S. Geological Survey Water-Resources Investigations Report 88–4153, 310 p.

Protocol (2020). *Sorption Testing for Se, Tc, Np, U and Eu on Crystalline Rocks*. Nuclear Waste Management Organization

Qiang Jin, Gang Wang, Mengtuan Ge, Zongyuan Chen, Wangsuo Wu, Zhijun Guo. (2014). *The adsorption of Eu(III) and Am(III) on Beishan granite: XPS, EPMA, batch and modeling study*. Applied Geochemistry, Volume 47, 2014, Pages 17-24, ISSN 0883-2927,

R. Guillaumont, T. Fanghnel, V. Neck, J. Fuger, D.A. Palmer, I. Grenthe, M.H. Rand (2003). *Update on the Chemical Thermodynamics of Uranium, Neptunium, Plutonium, Americium and Technetium*. OECD Nuclear Energy Agency, Issy-les-Moulineaux, France

Riddoch, J. (2016). *Sorption of Palladium onto Bentonite, Illite and Shale Under High Ionic Strength Conditions*. McMaster University, MASc Thesis.

Sheng, G. D., Shao, Dadong D., Fan, Qiao Hui, Xu, Di, Chen, Y. X. and Wang, X. K. (2009). *Effect of pH and ionic strength on sorption of Eu(III) to MX-80 bentonite: batch and XAFS study*. rca - Radiochimica Acta, vol. 97, no. 11, 2009, pp. 621-630.

Shinya, Nagasaki. (2018). *Sorption Properties of Np on Shale, Illite and Bentonite Under Saline, Oxidizing and Reducing Conditions.* Nuclear Waste Management Organization. NWMO-TR-2018-02.

Spahiu, K, and Bruno, J. (1995). *A selected thermodynamic database for REE to be used in HLNW performance assessment exercises*. Sweden: N. p.

Stumm, W., & Morgan, J. J. (1995). *Aquatic chemistry: Chemical equilibria and rates in natural waters*. ProQuest Ebook Central.

Tao Yu, Wang Suo Wu, Qiao Hui Fan. (2012). *Sorption of Am(III) on Na-bentonite: Effect of pH, ionic strength, temperature and humic acid*, Chinese Chemical Letters, Volume 23, Issue 10, 2012, Pages 1189-1192, ISSN 1001-8417,

Tao Yu, Zheting Xu, Jianhua Ye. (2019). *Adsorption kinetics of Eu(III) and Am(III) onto bentonite: analysis and application of the liquid membrane tidal diffusion model.* J Radioanal Nucl Chem 319, 749–757.

Tertre E., Berger G., Simoni E., Castet S., Giffaut E., Loubet M., Catalette H. (2006). *Europium retention onto clay minerals from 25 to 150 °C: Experimental measurements, spectroscopic features and sorption modelling*. Geochimica et Cosmochimica Acta, 70 (18) , pp. 4563-4578.

Thomas Rabung, Horst Geckeis, Jae-Il Kim, Horst Philipp Beck. (1998). *Sorption of Eu(III) on a Natural Hematite: Application of a Surface Complexation Model, Journal of Colloid and Interface Science*, Volume 208, Issue 1, 1998, Pages 153-161, ISSN 0021-9797,

Thorstenson, D.C., and Parkhurst, D.L. (2002), *Calculation of individual isotope equilibrium*

constants for implementation in geochemical models: U.S. Geological Survey Water-Resources Investigations Report 2002–4172, 129 p.

Truesdell, A. and Jones, B. F. (1974). *WATEQ, A Computer Program for Calculating Chemical Equilibria in Natural Waters*. U. S. Geological Survey Journal of Research, 2, 233{248.

U.S. Environmental Protection Agency, (1999), *MINTEQA2/PRODEFA2, A geochemical assessment model for environmental systems—User manual supplement for version 4.0*: Athens, Georgia, National Exposure Research Laboratory, Ecosystems Research Division, 76 p. Revised September 1999.

Wanqiang Zhou, Yanlin Shi, Yao Li, Dongfan Xian, Jingyi Wang, Chunli Liu, (2021). Adsorption of Eu(III) at rutile/water interface: Batch, spectroscopic and modelling studies, Colloids and Surfaces A: Physicochemical and Engineering Aspects, Volume 611, 2021, 125811, ISSN 0927-7757.

Wayne Robbins and Laurie Swami. (2020). Guided by science. Grounded in knowledge, committed to partnership. Annual report 2020. NWMO.

Xiangke Wang, Jinzhou Du, Zuyi Tao, and Zunhe Li. (2013). *Evaluation of Eu (III) migration in compacted bentonite*. Journal of Radioanalytical and Nuclear Chemistry, June 2013.

Xiangxue Wang, Yubing Sun, Ahmed Alsaedi, Tasawar Hayat, Xiangke Wang. (2015). *Interaction mechanism of Eu(III) with MX-80 bentonite studied by batch, TRLFS and kinetic desorption techniques,* Chemical Engineering Journal, Volume 264, 2015, Pages 570-576, ISSN 1385-8947,

Yong He, Yong-gui Chen, Wei-min Ye, Xin-xin Zhang. (2020). *Effect of contact time, pH, and temperature on Eu(III) sorption onto MX-80 bentonite,* Chemical Physics. 2020.

Yubing Sun, Jiaxing Li, Xiangke Wang, (2014). *RETRACTED: The retention of uranium and europium onto sepiolite investigated by macroscopic, spectroscopic and modeling techniques,* Geochimica et Cosmochimica Acta, volume. 140, Pages 621-643, ISSN 0016-7037

Yukio Tachi, Michael Ochs & Tadahiro Suyama (2014) *Integrated sorption and diffusion model for bentonite. Part 1: clay–water interaction and sorption modeling in dispersed systems,* Journal of Nuclear Science and Technology, 51:10, 1177-1190, DOI: 10.1080/00223131.2014.914452

Zhao Sun, Yong-gui Chen, Yu-jun Cui, and Wei-min Ye. (2019). *Adsorption of Eu(III) onto Gaomiaozi bentonite corroded by cement waters: Effect of cement solutions on the long-term sorption performance of bentonite in the repository conditions*. Journal of Cleaner Production.

Zhijun Guo, Jiang Xu, Keliang Shi, Yuqin Tang, Wangsuo Wu, Zuyi Tao. (2009). *Eu(III) adsorption/desorption on Na-bentonite: Experimental and modeling studies*. Colloids and Surfaces A: Physicochemical and Engineering Aspects, Volume 339, Issues 1–3, 2009, Pages 126-133, ISSN 0927-7757,